Zoological Studies **64:**11 (2025)
doi:10.6620/ZS.2025.64-11

Zoological Studies

Open Access

Integrative Taxonomy Uncovers Four New Species and One New Record of Land Hermit Crabs *Coenobita* Latreille, 1829 (Crustacea: Decapoda: Anomura: Coenobitidae) from Indonesia

Hsi-Te Shih[1,§,*], Dwi Listyo Rahayu[2,§], and Félix Adhi Pramono[3]

[1]*Department of Life Science and Global Change Biology Research Center, National Chung Hsing University, Taichung 402, Taiwan. *Correspondence: E-mail: htshih@dragon.nchu.edu.tw (Shih)*
[2]*Research Center for Marine and Land Bioindustry, National Research and Innovation Agency, Dusun Teluk Kodek, Pemenang, Lombok Utara 83756, NTB, Indonesia. E-mail: dwilistyo@yahoo.com (Rahayu)*
[3]*Jalan Kacang Polong I #29, Bojong Indah, Rawabuaya - Cengkareng, Jakarta Barat 11740, Indonesia. E-mail: felixjw@hotmail.com (Pramono)*

urn:lsid:zoobank.org:pub:D2750620-CE61-48C7-9333-D2C43EAB5067
[§]HTS and DLR contributed equally to this paper.
Received 26 July 2024 / Accepted 24 February 2025 / Published -- 2025
Communicated by Benny K.K. Chan

In this study, four new species of land hermit crabs (Crustacea: Decapoda: Anomura: Coenobitidae: *Coenobita* Latreille, 1829) are described from Indonesia. These descriptions are based on evidence from morphological differences as well as mitochondrial 16S rDNA and cytochrome *c* oxidase subunit I data. Among the new species, *Coenobita moluccensis* n. sp. (from Aru Island, Maluku), *C. patsyae* n. sp. (from Central Sulawesi and Southeast Sulawesi), and *C. celebensis* n. sp. (from Central Sulawesi) form a major clade on the phylogenetic tree, exhibiting similarities in morphology, particularly in the male sexual tubes—a character they share with their closely related counterpart, *C. lila* Rahayu, Shih & Ng, 2016. Although the four species are similar in overall morphology, they can be distinguished by differences in the left third pereopod, the second article of the antennal peduncles, granulation on the pereopods, as well as their live coloration. *Coenobita granularis* n. sp., found in Central Sulawesi, shares morphological similarities with the genetically closely related *C. pseudorugosus* Nakasone, 1988, particularly in the male sexual tubes. However, the two species can be distinguished by differences in the morphology of the male sexual tubes, the presence of tubercles on the left cheliped, the left third pereopod, as well as their live coloration. Additionally, a newly recorded species, *C. variabilis* McCulloch, 1909, has been confirmed in West Papua. This study brings the total number of *Coenobita* species known from Indonesia to 13.

Key words: *Coenobita moluccensis*, *C. patsyae*, *C. celebensis*, *C. variabilis*, New species, Newly recorded species, Morphology, 16S rDNA, Cytochrome *c* oxidase subunit I (*COI*), Phylogeny

BACKGROUND

The genus *Coenobita* contains 17 species, distributed throughout the tropical and subtropical zones of the world, including the Indo-West Pacific (IWP) and Atlantic-East Pacific (AEP) regions (Hartnoll 1988; McLaughlin et al. 2010; Rahayu et al. 2016; Shih et al. 2023a). In the Coral Triangle region (approximately corresponding to the ranges of the Malay Archipelago or the Indo-Australian Archipelago [IAA], depending

Citation: Shih HT, Rahayu DL, Pramono FA. 2025. Integrative taxonomy uncovers four new species and one new record of land hermit crabs *Coenobita* Latreille, 1829 (Crustacea: Decapoda: Anomura: Coenobitidae) from Indonesia. Zool Stud **64:**11. doi:10.6620/ZS.2025.64-11.

on the definition; Hoeksema 2007; Lohman et al. 2011), this genus exhibits the highest species diversity, with up to eight species recorded: *C. brevimanus* Dana, 1852, *C. cavipes* Stimpson, 1858, *C. lila* Rahayu, Shih & Ng, 2016, *C. longitarsis* De Man, 1902, *C. perlatus* H. Milne Edwards, 1837, *C. pseudorugosus* Nakasone, 1988, *C. rugosus* H. Milne Edwards, 1837, and *C. violascens* Heller, 1862 (Nakasone 1988; Shih 2012 2020; Rahayu et al. 2016; Shih et al. 2023a). This high species diversity is consistent with patterns seen in other coastal organisms in the Coral Triangle, *e.g.*, corals, shrimps, gastropods, and reef fishes (De Grave 2001; Hoeksema 2007; Bellwood and Meyer 2009; Veron et al. 2009).

Indonesia is a biodiversity hotspot, boasting the highest marine species diversity among countries within the Coral Triangle, and many marine species remain undescribed (Veron et al. 2009; Siallagan et al. 2023). Currently, all eight species of *Coenobita* mentioned above have been recorded in Indonesia (Wáng 2006; Rahayu et al. 2016; Shih et al. 2023a). In recent years, one of the authors (F.A. Pramono) collected specimens of *Coenobita* from the Indonesian coast and observed some individuals displaying distinctive coloration and morphology that warranted further study to clarify their species identity.

After a detailed examination of their morphology and analyses of molecular data from cytochrome *c* oxidase subunit I (*COI*), four new species and one newly recorded species from Indonesia have been confirmed. Three of the new species belong to the group lacking a stridulatory ridge, while one new species possesses a stridulatory ridge on the outer palm of the left chela. These four species differ from their congeners in several morphological characters, including the left cheliped, the left third pereopods, the second article of the antennal peduncles, the male sexual tubes, and the live coloration. The new record is *C. variabilis* McCulloch, 1909, which was originally thought to be endemic to Australia.

MATERIALS AND METHODS

Specimens examined or sequenced were deposited in the Museum Zoologi Bogor (MZB), National Research and Innovation Agency (= Badan Riset dan Inovasi Nasional, BRIN), Cibinong, Indonesia; the Zoological Collections of the Department of Life Science, National Chung Hsing University (NCHUZOOL), Taichung, Taiwan; the Florida Museum of Natural History, University of Florida, Florida, USA (UF); and the Zoological Reference Collection (ZRC) of the Lee Kong Chian Natural History, National University of Singapore, Singapore.

Morphological characters were illustrated with the aid of a drawing tube attached to a stereomicroscope. Descriptive terminology followed that of McLaughlin et al. (2007) and Rahayu et al. (2016). The abbreviations P2, P3, P4, and P5 refer to the second, third, fourth, and fifth pereopods, respectively. Specimen size is indicated by shield length (SL) in mm, measured from the tip of the rostrum or midpoint of the rostral lobe to the midpoint of the posterior margin of the shield. The length of the ocular peduncles was measured along the left ultimate peduncular segment, including the cornea, along its lateral surface; and corneal diameter represents the maximum width of the cornea measured on the dorsal surface. Since *C. moluccensis*, *C. patsyae*, and *C. celebensis* are similar in morphology, a full description is provided only for *C. moluccensis*. However, a Diagnosis section is included for each species (see the example in Shih et al. 2023c).

Genomic DNA was isolated from gill or muscle tissue using kits (see Shih et al. 2016 for details). A region of approximately 545 basepairs (bp) from the 5'-end of the mitochondrial large ribosomal subunit (16S rDNA) gene was selected for amplification with polymerase chain reaction (PCR) using the primers 1471, 1472 (Crandall and Fitzpatrick 1996), 16L29, 16H10, and 16H11 (Schubart 2009), as well as the newly designed primers, 16L29B (5'-YGCCTGTTTAYCAAAAACAT-3') and 16H10B (5'-AATCCTTTCGTACTARR-3'). A portion of the *COI* gene was amplified using PCR with the primers LCO1490, HCO2198 (Folmer et al. 1994), LCOB, HCOex3 (Shih et al. 2022), LCOC, HCOex4 (Shih et al. 2023a), HCOex0 (Shih et al. 2023b), LCOex2, and LCOex3 (Shih et al. 2023d), as well as the newly designed primer, HCOex1 (5'-GCYTCTTTYTTDCCMGACTC-3'). PCR conditions for the above primers involved 40 cycles of denaturation for 50 s at 94°C, annealing for 70 s at 45–47°C, and extension for 60 s at 72°C, followed by a final extension for 10 min at 72°C. Sequences were obtained by automated Sanger sequencing (Applied Biosystems 3730, USA). Sequences of the different haplotypes were deposited in NCBI GenBank (accession numbers are shown in Table 1). Additional *COI* sequences published in Rahayu et al. (2016) and Shih et al. (2023a) were also included (Table 1). Sequences were aligned using the MUSCLE function in MEGA (vers. 11, Tamura et al. 2021).

For the combined 16S and *COI* dataset, the best-fitting models for sequence evolution of individual datasets were determined by PartitionFinder (vers. 2.1.1, Lanfear et al. 2017), using the Bayesian information criterion (BIC). The best model, HKY+I+G, was

subsequently applied for maximum likelihood (ML) and Bayesian inference (BI) analyses. The ML analysis was conducted in IQ-TREE (vers. 2.2.0, Minh et al. 2020) with the best models and 30,000 ultrafast bootstrap replicates (Hoang et al. 2017). The BI was performed with MrBayes (vers. 3.2.6, Ronquist et al. 2012). The search was run with four chains for 10 million generations and four independent runs, with trees sampled every 1000 generations. The convergence of chains was determined by the average standard deviation of split frequency values below the recommended 0.01 (Ronquist et al. 2020), and the first 3500 trees were discarded as the burnin. A TCS haplotype network of the 16S+*COI* haplotypes was generated using the program PopART (vers. 1.7, Leigh and Bryant 2015). For barcoding *COI*, basepair (bp) differences and pairwise estimates of Kimura 2-parameter (K2P) distances (Kimura 1980) for genetic diversities between *COI* haplotypes were calculated with MEGA.

Comparative material: ***Coenobita cavipes* Stimpson, 1858**: 1 ♂ (12.4 mm) (ZRC 2013.0267), Manado, Sulawesi, Coll. N.K. Ng, 25 Sep. 2003; 1 ♂ (11.3 mm) (MZB Cru 5724), Ajkwa, Papua, 29 September 2021; 1 ♂ (20.0 mm), Malalayang, Manado, Sulawesi, coll. N.K. Ng, 14 Apr. 2003. ***C. lila* Rahayu, Shih & Ng, 2016**: 1 paratype ♂ (10.7 mm) (NCHUZOOL 13624); 1 ♂ (11.3 mm) (NCHUZOOL 15284), St John's Island, coll. H-T Shih et al., 10 Feb. 2014; 10 ♂♂ (3.8–11.3 mm), 1 ♀ (4.6 mm), 1 ovig. ♀ (9.0 mm, St John's Island, Singapore, 10 February 2014; 10 ♂♂ (3.8–11.3 mm), 1 ♀ (4.6 mm), 1 ovig. ♀ (9.0 mm) (ZRC 2013.1782) St 78, St John's Island, 25 May 2013. ***C. perlatus* H. Milne Edwards, 1837**: 2 ♂♂ (10.3, 10.9 mm) (NCHUZOOL 17213), 1 ♀ (13.5 mm) (NCHUZOOL 17230), Pago Bay, Guam, 4 Aug. 2001. ***C. pseudorugosus* Nakasone, 1988**: Central Sulawesi, Indonesia: 2 ♂♂ (13.0, 14.2 mm) (NCHUZOOL 17199), Oct. 2022; 6 ♂♂ (8.0–13.8 mm) (NCHUZOOL 17200), Dec. 2022; 5 ♂♂ (9.1–12.7 mm) (NCHUZOOL 17201), Dec. 2022. ***C. purpureus* Stimpson, 1858**: Japan (purchased): 1 ♂, 22.1 mm (NCHUZOOL 17215), 1 ♂ (21.6) mm (NCHUZOOL 17216), 1 ♀, 18.6 mm (NCHUZOOL 17217). ***C. scaevola* (Forskål, 1775)**: Djibouti: 3 ♂♂ (8.3–10.2 mm), 2 ♀♀ (7.9, 9.0 mm) (UF 33344), Moucha Islands, Maskali Bank, Sunken Buoy dive site, 27 Sep. 2012; Oman: 2 ♂♂ (17.5, 17.9 mm), 5 ♀♀ (14.8–18.4 mm) (UF 7609), Bar al Hikman peninsula, E side shore of peninsula, 19 Jan. 2005; Iran: 1 ♂ (16.8 mm), 1 ♀ (11.9 mm) (ZRC 2017.0642), Djod Village, Gulf of Oman, coll. S. Ebrahimnezhad, Oct. 2014.

RESULTS

TAXONOMY

Family Coenobitidae Dana, 1851
Genus *Coenobita* Latreille, 1829
Coenobita moluccensis n. sp.

(Figs. 1–4, 13A, B)

urn:lsid:zoobank.org:act:6591BEEE-2971-41AF-909F-192976A23B26

Material examined: Holotype: ♂ (12.0 mm) (MZB Cru 5722), Aru Island, Maluku, coll. local

Table 1. Haplotypes of 16S rDNA and cytochrome *c* oxidase subunit I (*COI*) genes of *Coenobita* species used in this study. *, holotype; **, paratype. See MATERIALS AND METHODS for abbreviations of museums and universities

Species	Locality	Catalog no. (or tissue sample [TS] code)	Sample size	Haplotype of 16S	Access. no. of 16S	Haplotype of *COI*	Access. no. of *COI*
C. brevimanus	Taiwan: Dongsha I.	NCHUZOOL 17212	1	Cbr	PQ427321	Cbr_C1	OR413746
	Philippines: Olango I., Cebu	UF 3799	1	Cbr	PQ427322	Cbr_C2	OR413747
	Thailand: Similan	ZRC SM-03	1	Cbr	PQ427323	Cbr_C3	OR413748
C. cavipes	Taiwan: Lyudao, Taitung	NCHUZOOL 13625	1	Cca1	PQ427324	Cca_C1	AB998653
	Taiwan: Lyudao, Taitung	NCHUZOOL 13626	1	Cca1	PQ427325	Cca_C2	AB998654
	Taiwan: Houwan, Kenting	NCHUZOOL 13627	1	Cca2	PQ427326	Cca_C3	AB998655
	Taiwan: Yuanjhonggang, Kaohsiung	NCHUZOOL 13628	1	Cca1	PQ427327	Cca_C4	AB998656
	Philippines: Kawasan Falls, Cebu	UF 11345	1	Cca3	PQ427328	Cca_C5	AB998657
C. lila	Singapore: St John's I.	NCHUZOOL 13635	1	Cli1	PQ427329	Cli_C1	AB998648
	Singapore: Pulau Jong	NCHUZOOL 13636	1	Cli2	PQ427330	Cli_C2	AB998649
C. longitarsis	Papua New Guinea	UF 11434	1	Clo1	PQ427331	Clo_C1	OR413749
	Papua New Guinea	UF 11438	1	Clo2	PQ427332	Clo_C2	OR413750
	Papua New Guinea	UF 11435	1	Clo3	PQ427333	Clo_C3	OR413751
	Papua New Guinea	UF 11436	1	Clo3	PQ427334	Clo_C4	OR413752

Table 1. (Continued)

Species	Locality	Catalog no. (or tissue sample [TS] code)	Sample size	Haplotype of 16S	Access. no. of 16S	Haplotype of *COI*	Access. no. of *COI*
C. perlatus	Guam	NCHUZOOL 17213	1	Cpe	PQ427335	Cpe_C1	OR413753
	Christmas Island	ZRC CI-D07-2011	1	Cpe	PQ427336	Cpe_C2	OR413754
	Taiwan: Taiping I.	NCHUZOOL 17214	1	Cpe	PQ427337	Cpe_C3	OR413755
C. pseudorugosus	Philippines: Panglao, Bohol	UF 13164	1	Cps1	PQ427338	Cps_C1	OR413757
	Philippines: Camiguin	NCHUZOOL 17197	1	Cps1	PQ427339	Cps_C2	OR413760
	Indonesia: Central Sulawesi: Gulf of Tomini	NCHUZOOL 17201	1	Cps2	PQ427340	Cps_C3	OR413768
	Indonesia: Central Sulawesi: Gulf of Tomini	NCHUZOOL 17200	1	Cps1	PQ427341	Cps_C4	OR413770
C. purpureus	purchased	NCHUZOOL 17215	1	Cpu1	PQ427342	Cpu_C1	OR413775
	purchased	NCHUZOOL 17216	1	Cpu2	PQ427343	Cpu_C2	OR413776
	purchased	NCHUZOOL 17217	1	Cpu3	PQ427344	Cpu_C3	OR413777
C. rugosus	Taiwan: Taiping I.	NCHUZOOL 17204	1	Cru1	PQ427345	Cru_C1	OR413778
	Philippines: Camiguin	NCHUZOOL 17218	1	Cru2	PQ427346	Cru_C2	OR413779
	Christmas I.	ZRC	1	Cru3	PQ427347	Cru_C3	OR413780
C. spinosus	Niue	UF 2449	1	Csp1	PQ427348	Csp_C1	OR413781
	Vanuatu	UF 7501	1	Csp2	PQ427349	Csp_C2	OR413782
	Wallis and Futuna	NCHUZOOL 17216	1	Csp2	PQ427350	Csp_C3	OR413783
C. variabilis	Australia: West Governor I., WA	QM W21232	1	Cva1	PQ427351	Cva_C1	PQ426898
	Australia: West Governor I., WA	QM W21232	1	Cva2	PQ427352	Cva_C2	PQ426899
	Australia: West Governor I., WA	QM W21232	1	Cva2	PQ427353	Cva_C3	PQ426900
	Indonesia: West Papua	NCHUZOOL 15257	2	Cva3	PQ427354, PQ427355	Cva_C4	PQ426901, PQ426902
	Indonesia: West Papua	NCHUZOOL 15258	2	Cva3	PQ427356, PQ427357	Cva_C5	PQ426903, PQ426904
C. violascens	Taiwan: Yuanjhonggang, Kaohsiung	NCHUZOOL 13629	1	Cvi	PQ427358	Cvi_C1	AB998658
	Taiwan: Yuanjhonggang, Kaohsiung	NCHUZOOL 13630	1	Cvi	PQ427359	Cvi_C2	AB998659
	Taiwan: Dongsha I., Kaohsiung	NCHUZOOL 13631	1	Cvi	PQ427360	Cvi_C3	AB998660
	Taiwan: Dongsha I., Kaohsiung	NCHUZOOL 13632	1	Cvi	PQ427361	Cvi_C4	AB998661
	Philippines: Kawasan Falls, Cebu	UF 11347	1	Cvi	PQ427362	Cvi_C5	AB998664
C. moluccensis	Indonesia: Aru, Maluku	(TS COx94)	1	Cmo1	PQ427363	Cmo_C1	PQ426905
	Indonesia: Aru, Maluku	(TS COx100)	1	Cmo2	PQ427364	Cmo_C2	PQ426906
	Indonesia: Aru, Maluku	NCHUZOOL 15259**	1	Cmo2	PQ427365	Cmo_C2	PQ426907
	Indonesia: Aru, Maluku	(TS COx101)	1	Cmo3	PQ427366	Cmo_C4	PQ426908
	Indonesia: Aru, Maluku	(TS COx102)	1	Cmo4	PQ427367	Cmo_C5	PQ426909
	Indonesia: Aru, Maluku	(TS COx103)	1	Cmo5	PQ427368	Cmo_C6	PQ426910
	Indonesia: Aru, Maluku	(TS COx104)	1	Cmo6	PQ427369	Cmo_C7	PQ426911
	Indonesia: Aru, Maluku	(TS COx105)	1	Cmo7	PQ427370	Cmo_C8	PQ426912
	Indonesia: Aru, Maluku	MZB Cru 5722*	1	Cmo7	PQ427371	Cmo_C8	PQ426913
	Indonesia: Aru, Maluku	(TS COx106)	1	Cmo4	PQ427372	Cmo_C9	PQ426914
	Indonesia: Aru, Maluku	MZB Cru 5723**	1	Cmo4	PQ427373	Cmo_C9	PQ426915
	Indonesia: Aru, Maluku	MZB Cru 5723**	1	Cmo4	PQ427374	Cmo_C9	PQ426916
	Indonesia: Aru, Maluku	ZRC 2023.0252**	1	Cmo4	PQ427375	Cmo_C9	PQ426917
	Indonesia: Aru, Maluku	MZB Cru 5723**	1	Cmo2	PQ427376	Cmo_C10	PQ426918
	Indonesia: Aru, Maluku	ZRC 2023.0252**	1	Cmo9	PQ427377	Cmo_C11	PQ426919
	Indonesia: Aru, Maluku	NCHUZOOL 15259**	1	Cmo8	PQ427378	Cmo_C3	PQ426920
C. patsyae	Indonesia: Central Sulawesi	(TS COx87)	1	Cpa1	PQ427379	Cpa_C1	PQ426921
	Indonesia: Central Sulawesi	(TS COx88)	1	Cpa2	PQ427380	Cpa_C2	PQ426922
	Indonesia: Central Sulawesi	(TS COx89)	1	Cpa1	PQ427381	Cpa_C3	PQ426923
	Indonesia: Central Sulawesi	(TS COx90)	1	Cpa3	PQ427382	Cpa_C4	PQ426924
	Indonesia: Central Sulawesi	(TS COx91)	1	Cpa4	PQ427383	Cpa_C5	PQ426925
	Indonesia: Central Sulawesi	(TS COx92)	1	Cpa5	PQ427384	Cpa_C6	PQ426926
	Indonesia: Central Sulawesi: Gulf of Tomini	MZB Cru 5725*	1	Cpa6	PQ427385	Cpa_C7	PQ426927
	Indonesia: Central Sulawesi	NCHUZOOL 15271	1	Cpa6	PQ427386	Cpa_C7	PQ426928

Table 1. (Continued)

Species	Locality	Catalog no. (or tissue sample [TS] code)	Sample size	Haplotype of 16S	Access. no. of 16S	Haplotype of *COI*	Access. no. of *COI*
	Indonesia: Southeast Sulawesi	NCHUZOOL 15272	2	Cpa6	PQ427387, PQ427388	Cpa_C7	PQ426929, PQ426930
	Indonesia: Central Sulawesi	NCHUZOOL 15275	1	Cpa6	PQ427389	Cpa_C7	PQ426931
	Indonesia: Central Sulawesi: Gulf of Tomini	MZB Cru 5726**	1	Cpa2	PQ427390	Cpa_C8	PQ426932
	Indonesia: Central Sulawesi: Gulf of Tomini	ZRC 2023.0254**	1	Cpa2	PQ427391	Cpa_C9	PQ426933
	Indonesia: Central Sulawesi: Gulf of Tomini	ZRC 2023.0254**	1	Cpa2	PQ427392	Cpa_C10	PQ426934
	Indonesia: Central Sulawesi: Gulf of Tomini	ZRC 2023.0254**	1	Cpa8	PQ427393	Cpa_C11	PQ426935
	Indonesia: Central Sulawesi	NCHUZOOL 15271	1	Cpa9	PQ427394	Cpa_C12	PQ426936
	Indonesia: Central Sulawesi	NCHUZOOL 15271	1	Cpa10	PQ427395	Cpa_C13	PQ426937
	Indonesia: Central Sulawesi	NCHUZOOL 15271	1	Cpa7	PQ427396	Cpa_C14	PQ426938
	Indonesia: Central Sulawesi	NCHUZOOL 15271	1	Cpa11	PQ427397	Cpa_C15	PQ426939
	Indonesia: Southeast Sulawesi	NCHUZOOL 15272	1	Cpa12	PQ427398	Cpa_C16	PQ426940
	Indonesia: Southeast Sulawesi	NCHUZOOL 15272	1	Cpa13	PQ427399	Cpa_C17	PQ426941
	Indonesia: Southeast Sulawesi	NCHUZOOL 15272	1	Cpa13	PQ427400	Cpa_C15	PQ426942
	Indonesia: Southeast Sulawesi	NCHUZOOL 15272	1	Cpa14	PQ427401	Cpa_C18	PQ426943
	Indonesia: Southeast Sulawesi	NCHUZOOL 15272	1	Cpa7	PQ427402	Cpa_C19	PQ426944
	Indonesia: Central Sulawesi	NCHUZOOL 15275	1	Cpa7	PQ427403	Cpa_C19	PQ426945
	Indonesia: Central Sulawesi	NCHUZOOL 15273	1	Cpa15	PQ427404	Cpa_C20	PQ426946
	Indonesia: Southeast Sulawesi	NCHUZOOL 15274	1	Cpa6	PQ427405	—	
	Indonesia: Central Sulawesi	NCHUZOOL 15275	1	Cpa6	PQ427406	Cpa_C21	PQ426947
	Indonesia: Central Sulawesi: Gulf of Tomini	NCHUZOOL 15278	1	Cpa1	PQ427407	Cpa_C22	PQ426948
	Indonesia: Central Sulawesi: Gulf of Tomini	NCHUZOOL 15278	1	Cpa2	PQ427408	Cpa_C23	PQ426949
	Indonesia: Central Sulawesi: Gulf of Tomini	NCHUZOOL 15278	1	Cpa2	PQ427409	Cpa_C24	PQ426950
	Indonesia: Central Sulawesi: Gulf of Tomini	NCHUZOOL 15278	1	Cpa1	PQ427410	Cpa_C25	PQ426951
	Indonesia: Central Sulawesi: Gulf of Tomini	NCHUZOOL 15280	1	Cpa1	PQ427411	Cpa_C26	PQ426952
	Indonesia: Central Sulawesi: Gulf of Tomini	NCHUZOOL 15280	1	Cpa1	PQ427412	Cpa_C27	PQ426953
	Indonesia: Central Sulawesi: Gulf of Tomini	NCHUZOOL 15280; MZB Cru 5726**	2	Cpa7	PQ427413, PQ427414	Cpa_C28	PQ426954, PQ426955
C. celebensis	Indonesia: Central Sulawesi: Gulf of Tomini	MZB Cru 5727*	1	Cce1	PQ427415	Cce_C1	PQ426956
	Indonesia: Central Sulawesi: Gulf of Tomini	ZRC 2024.0263**	1	Cce1	PQ427416	Cce_C1	PQ426957
	Indonesia: Central Sulawesi: Gulf of Tomini	MZB Cru 5728**	1	Cce1	PQ427417	Cce_C2	PQ426958
	Indonesia: Central Sulawesi: Gulf of Tomini	MZB Cru 5728**	1	Cce1	PQ427418	Cce_C3	PQ426959
	Indonesia: Central Sulawesi: Gulf of Tomini	ZRC 2024.0263**	1	Cce1	PQ427419	Cce_C4	PQ426960
	Indonesia: Central Sulawesi	NCHUZOOL 15276**	1	Cce2	PQ427420	Cce_C5	PQ426961
	Indonesia: Central Sulawesi	NCHUZOOL 15277**	1	Cce1	PQ427421	Cce_C6	PQ426962
	Indonesia: Central Sulawesi: Gulf of Tomini	NCHUZOOL 15279**	1	Cce1	PQ427422	Cce_C7	PQ426963
	Indonesia: Central Sulawesi: Gulf of Tomini	NCHUZOOL 15281**	1	Cce1	PQ427423	Cce_C8	PQ426964
C. granularis	Indonesia: Central Sulawesi	(TS COx95)	1	Cgr1	PQ427424	Cgr_C1	PQ426965
	Indonesia: Central Sulawesi	(TS COx96)	1	Cgr1	PQ427425	Cgr_C2	PQ426966
	Indonesia: Central Sulawesi	(TS COx97)	1	Cgr1	PQ427426	Cgr_C3	PQ426967
	Indonesia: Central Sulawesi	(TS COx98)	1	Cgr1	PQ427427	Cgr_C4	PQ426968
	Indonesia: Central Sulawesi	(TS COx99)	1	Cgr2	PQ427428	Cgr_C5	PQ426969
	Indonesia: Central Sulawesi: Gulf of Tomini	MZB Cru 5729*	1	Cgr3	PQ427429	Cgr_C6	PQ426970
	Indonesia: Central Sulawesi: Gulf of Tomini	MZB Cru 5730**	1	Cgr5	PQ427430	Cgr_C7	PQ426971
	Indonesia: Central Sulawesi: Gulf of Tomini	MZB Cru 5791	1	Cgr5	PQ427431	Cgr_C6	PQ426972
	Indonesia: Central Sulawesi: Gulf of Tomini	MZB Cru 5791	1	Cgr4	PQ427432	Cgr_C8	PQ426973
	Indonesia: Central Sulawesi: Gulf of Tomini	MZB Cru 5791	1	Cgr1	PQ427433	Cgr_C9	PQ426974
	Indonesia: Central Sulawesi: Gulf of Tomini	ZRC 2023.0253	1	Cgr5	PQ427434	Cgr_C10	PQ426975
	Indonesia: Central Sulawesi: Gulf of Tomini	ZRC 2023.0253	1	Cgr5	PQ427435	Cgr_C11	PQ426976
	Indonesia: Central Sulawesi: Gulf of Tomini	ZRC 2024.0264**	1	Cgr1	PQ427436	Cgr_C12	PQ426977
	Indonesia: Central Sulawesi: Gulf of Tomini	ZRC 2024.0264**	1	Cgr1	PQ427437	Cgr_C13	PQ426978
	Indonesia: Central Sulawesi: Gulf of Tomini	NCHUZOOL 15254	1	Cgr1	PQ427438	Cgr_C14	PQ426979
	Indonesia: Central Sulawesi: Gulf of Tomini	NCHUZOOL 15254	1	Cgr1	PQ427439	Cgr_C15	PQ426980
	Indonesia: Central Sulawesi: Gulf of Tomini	NCHUZOOL 15254	1	Cgr1	PQ427440	Cgr_C16	PQ426981
	Indonesia: Central Sulawesi: Gulf of Tomini	NCHUZOOL 15255**	1	Cgr1	PQ427441	Cgr_C17	PQ426982
	Indonesia: Central Sulawesi: Gulf of Tomini	NCHUZOOL 15256	1	Cgr1	PQ427442	Cgr_C18	PQ426983
	Indonesia: Central Sulawesi: Gulf of Tomini	NCHUZOOL 15256	1	Cgr1	PQ427443	Cgr_C19	PQ426984

people, Dec. 2022. Paratypes: 2 ♂♂ (9.9, 14.6 mm), 1 ovig. ♀ (6.7 mm) (MZB Cru 5723), 3 ♂♂ (9.3, 11.3, 16.0 mm) (ZRC 2023.0252), 3 ♂♂ (10.5, 11.7, 14.4 mm) (NCHUZOOL 15259), same data as holotype.

Diagnosis: Shield (Figs. 1A, 4A–D) transversely convex, about 1.6 times as long as broad; dorsal surface with scattered small, flattened tubercles. Ocular peduncles reaching half length of fifth article of antennal peduncles; antennal peduncles reaching half length of penultimate article of antennular peduncles; antennular basal article 0.7 times as long as penultimate article (Fig. 1B); second article of antennal peduncle (Figs. 1C, 13A, B) stout, short. Chelipeds (Fig. 2A, B) unequal, dissimilar; left palm without stridulatory apparatus on upper outer surface; upper margin of palm of left and right cheliped with brush of long, coarse setae on proximal half; outer surface of palm of left cheliped with rows of tubercles, large and closely-set on upper half, smaller and fewer on lower half, some accompanied by tuft of very short setae; lower proximal part angled, forming broadly triangular lobe-like projection, continued to slightly upright lower margin of fixed finger. P2 and P3 dissimilar, P2 slightly shorter, more slender than P3; dactylus and propodus of left P2 (Fig. 3A, B) with small, sometimes corneous-tipped tubercles; ventral surface of dactylus with longitudinal ridge consisting of row of tiny corneous teeth; dactylus and propodus of right P2 covered with rows of corneous-tipped tubercles on lateral surface, larger tubercles on lower margin and ventral surface.

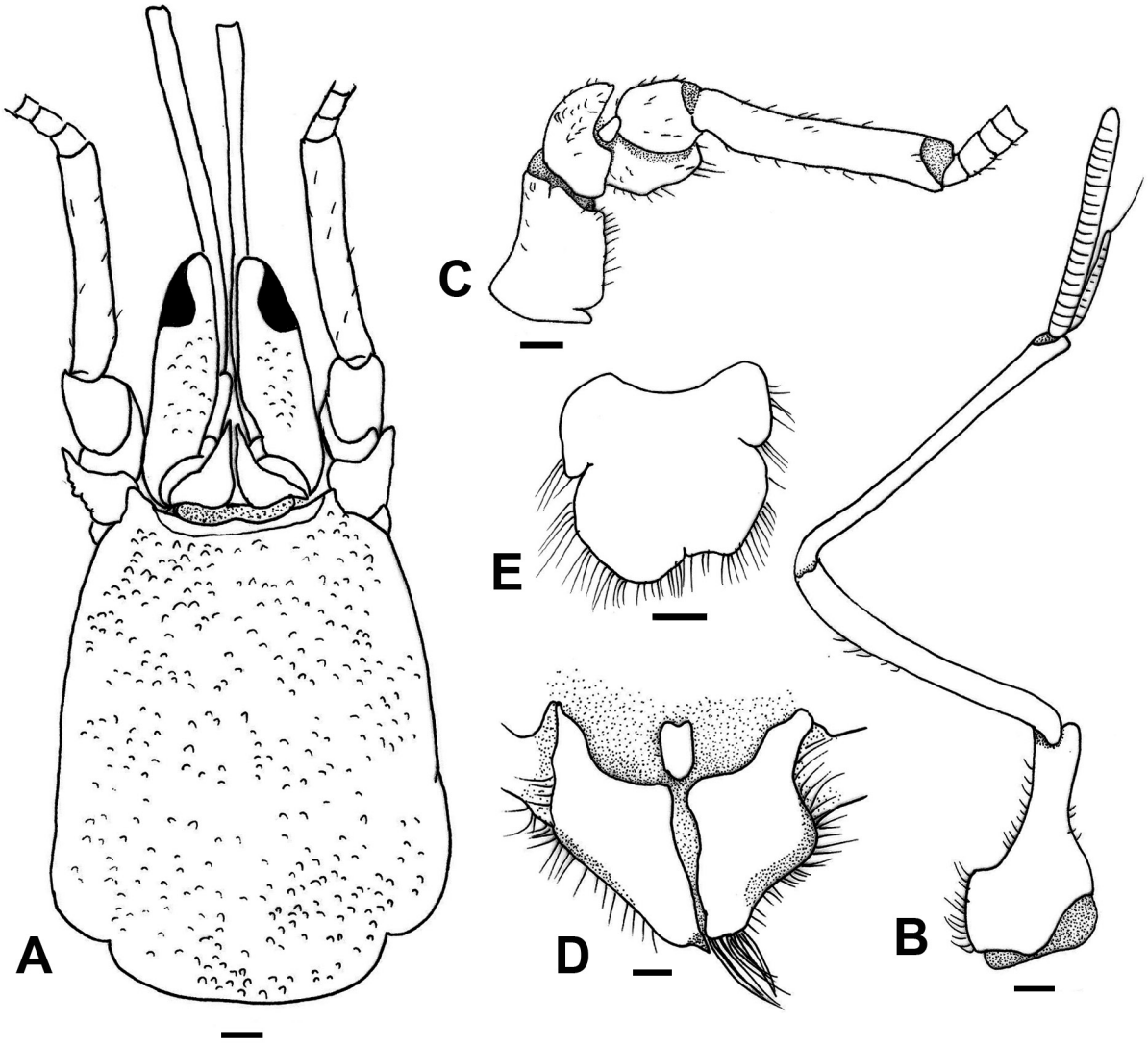

Fig. 1. *Coenobita moluccensis* n. sp. Holotype ♂ (SL 12.0 mm, MZB Cru 5722). A, shield and cephalic appendages; B, right antennular peduncles, lateral view; C, right antennal peduncles, lateral view; D, sternite and coxae of male P5; E, telson. Setae partially omitted. Scale bars: A = 2 mm; B–E = 1 mm.

Left P3 (Fig. 3C–E) with dactylus slightly convex laterally, punctate, with scattered short tufts of setae; ventral surface with longitudinal ridge consisting of row of widely-spaced tiny corneous teeth; lateral surface of propodus broad, slightly flattened distally, punctate or with flattened small tubercles; dorsal surface broader distally; right P3 (Fig. 3F, G) with dactylus and propodus with tubercles on lateral surface, ventral surface of dactylus with scattered corneous-tipped spines. P4 semi-chelate (Fig. 2C). In male, coxae of P5 (Figs. 1D, 2D) produced, thick, each forming moderately short, calcified sexual tube; moderately large, subquadrangular sternal protuberance between both coxae. Telson (Fig. 1E) with posterior lobes bearing very narrow median cleft.

Description: Shield (Figs. 1A, 4A–D) transversely convex, about 1.6 times as long as broad; anterior margin between rostrum and lateral projections slightly concave; lateral projection produced, terminating in pointed spine; posterior margin slightly rounded. Rostrum broadly rounded, obsolete. Lateral surface punctate; dorsal surface with scattered small, flattened tubercles.

Ocular peduncles compressed laterally, mesial surface shallowly concave distally, reaching half length of fifth article of antennal peduncles; cornea small, occupying only one-third of distal part of ocular peduncles laterally; dorsal surface with scattered small, flattened tubercles and sparse short setae. Ocular acicles triangular, terminating acutely.

Antennular peduncles (Fig. 1B) long. Basal article 0.7 times as long as penultimate article. Ultimate article longer than penultimate article. Upper rami of flagella stick-like, terminating in rounded tip, with very short setae on lateral and mesial margins, lower rami with 7 segments, long seta distally.

Antennal peduncles (Figs. 1C, 13A, B) exceeding ocular peduncles by half length of fifth article, reaching

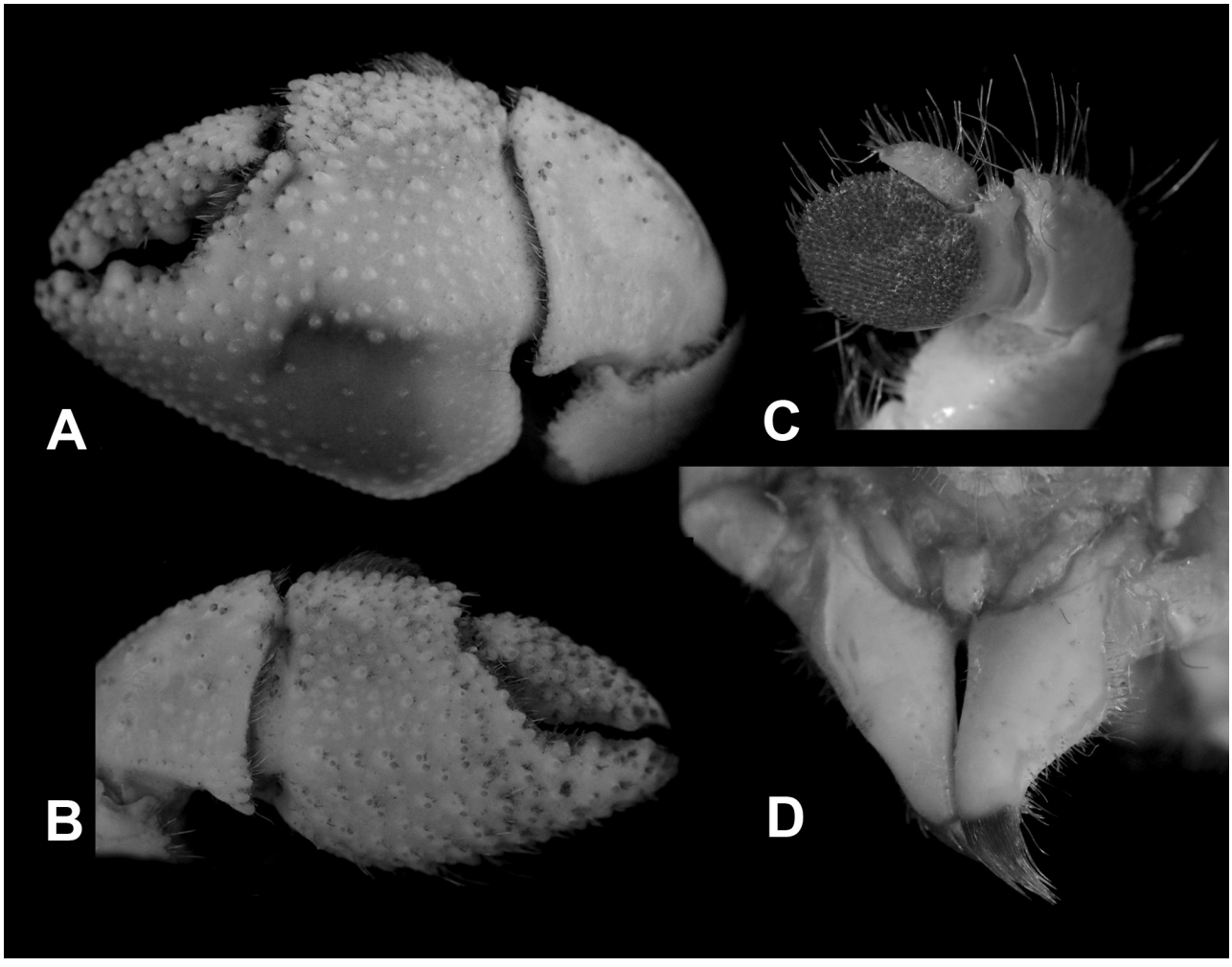

Fig. 2. *Coenobita moluccensis* n. sp. Holotype ♂ (SL 12.0 mm, MZB Cru 5722). A, left cheliped, outer view; B, right cheliped, outer view; C, left P4, lateral view; D, sternite and coxae of male P5.

half length of penultimate article of antennular peduncles. First article 1.3 times as long as broad. Second article stout, short, not reaching proximal area of fourth article, covered with small tubercles and sparse very short setae. Third to fifth articles unarmed, with scattered, very short setae. Antennal acicle fused to second article of peduncle. Flagella long, overreaching tip of right cheliped.

Chelipeds (Figs. 2A, B, 4A–D) unequal, dissimilar; left distinctly larger than right. Dactylus of left cheliped (Fig. 2A) longer than palm; outer surface with numerous large tubercles, with tufts of short setae, upper surface with large, flattened tubercles, inner surface with rows of corneous-tipped tubercles and tufts of very short, stiff setae; cutting edge with 1 large tooth proximally and distally, smaller tooth medially, terminating in small corneous claw. Fixed finger with sparse, tubercles on outer surface, some tubercles with 2 or 3 short setae; lower margin with row of tubercles, some with tufts of short setae; cutting edge with 2 large teeth and row of smaller teeth, terminating in small corneous claw; inner surface covered with large tubercles, each with short setae. Palm without stridulatory apparatus on upper outer surface, upper margin with row of large, tubercles, brush of long, coarse setae on proximal half; outer surface with rows of tubercles, large and closely-spaced on upper half, smaller and fewer on lower half, some accompanied by tuft of very short setae; lower margin with small, flattened tubercles bearing tufts of very short setae; lower proximal part angled, forming broadly triangular lobe-like projection, continued to slightly upright lower margin of fixed finger; inner surface with small and large tubercles, some with short and long setae, brush of setae proximally near upper margin. Carpus with sparse corneous-tipped tubercles on upper half of outer surfaces, each tubercle with tufts of setae, lower half smooth or with very low tubercles; inner surface with flattened tubercles, each tubercle accompanied with moderately long setae, long, setae on distal margin. Merus with transverse rows of flattened tubercles on outer surface; lower outer and inner margins each with tubercles and tufts of short setae, inner surface smooth.

Right cheliped (Fig. 2B) with dactylus longer than palm, outer surface covered with large, tubercles, some tubercles with corneous-tipped, inner surface with row of corneous-tipped tubercles and moderately long setae; cutting edge with row of moderately large teeth, terminating in small corneous claw. Fixed finger with cutting edge bearing several small teeth, large teeth adjacent terminal corneous claw and another in middle. Palm with thick brush of long coarse setae on upper margin; outer surface with rows of large tubercles, some with corneous-tipped, each with 2 or 3 long setae. Inner surface with scattered flattened tubercles, each with tufts of setae; proximal area of palm with long, coarse setae near upper margin. Carpus and merus similarly armed as left cheliped, but with long setae on lower margin of merus.

P2 and P3 dissimilar, P2 slightly shorter, more slender than P3. Dactylus of left P2 with lateral and dorsal surfaces flattened, covered with rows of corneous-tipped, tubercles, each with short stiff setae (Fig. 3A); mesial surface with rows of numerous corneous-tipped tubercles each bearing tufts of short setae; ventral surface (Fig. 3B) with longitudinal ridge consisting of row of tiny corneous teeth, ventrolateral margin with row of corneous-tipped tubercles and tufts of short setae. Propodus lateral surface covered with dense, small, sometimes corneous-tipped tubercles, each with 1 or 2 setae; dorsal surface broad, with row of small corneous-tipped tubercles; dorsomesial margin with row of large, corneous-tipped tubercles; mesial surface concave, smooth except for few small tubercles and setae, delimited ventrally by longitudinal row of small tubercles. Carpus with rows of large tubercles on dorsolateral margin, each bearing 2 or 3 short setae; lateral surface with sparse, small, corneous-tipped tubercles, each with tufts of setae; ventrolateral margin with larger corneous-tipped tubercles each with tufts of long setae; mesial surface concave with scattered tufts of short setae; ventromesial surface with sparse tufts of short setae. Merus compressed laterally and mesially, lateral and mesial surfaces smooth, except for several tubercles distolaterally.

Right P2 with dactylus covered with rows of corneous-tipped tubercles on lateral surface, larger tubercles on lower margin and ventral surface, dorsal margin not delimited, ventral surface with sparse corneous spines. Propodus, carpus and merus as in left P2.

Left P3 (Fig. 3C) with dactylus 1.3–1.5 times as long as propodus, lateral surface slightly convex distally, flattened or slightly concave proximally, punctate but with scattered short tufts of setae, delimited dorsally by row of small tubercles, sometimes corneous-tipped, bearing short setae, dorsal surface with longitudinal rows of corneous-tipped tubercles each with tufts of setae; tubercles on dorsal margin and dorsal surface decreasing in size proximally; mesial surface with rows of tubercles each with tufts of setae; ventrolateral margin with row tubercles, with corneous-tipped distally, each tubercles with long setae; ventral surface (Fig. 3D) slightly concave, median longitudinal ridge consisting of row of, widely-spaced, tiny corneous teeth. Propodus lateral surface broad, slightly flattened distally, slightly convex proximally, punctate or with flattened small tubercles; dorsolateral margin delimited

distally by row of small tubercles; dorsal surface (Fig. 3E) flattened, broadened distally, slightly narrowing proximally, with rows of small, flattened tubercles, each with very short setae, dorsomesial margin delimited by row of low tubercles, each with short setae; mesial surface slightly concave, with sparse tubercles, some with corneous-tipped, each with tufts of setae; ventral surface slightly flattened distally, concave proximally, with irregular rows of corneous-tipped tubercles, each with tufts of long setae; ventrolateral margin with row of small tubercles and tufts of sparse setae. Carpus with rows of tubercles, decreasing in size proximally, each with 2 or 3 short setae on dorsolateral margin, lateral surface with numerous corneous-tipped tubercles each with tufts of setae; ventrolateral margin with moderately large spines each with tufts of setae; mesial surface compressed, almost smooth except for few tufts of short setae. Merus compressed laterally and mesially, transverse row of flattened tubercles on lateral surface; mesial surface almost smooth, ventral margin with moderately large spines and tufts of long setae.

Right P3 more slender than left, with longer and denser setae on ventral margin. Dactylus and propodus (Fig. 3F, G) covered with tubercles, corneous-tipped tubercles mainly on dorso- and ventrolateral surfaces; dorsal margin not delimited; mesial surface of dactylus with rows of corneous-tipped tubercles and tufts of setae, ventral surface with sparse small corneous spines; mesial surface of propodus with sparse small tubercles and short setae. Carpus and merus as in left P3.

P4 semi-chelate (Fig. 2C). Dactylus with row of small corneous teeth ventrally, long, coarse setae dorsally; propodal rasp well developed, occupying large, semicircular area, consisting of numerous corneous

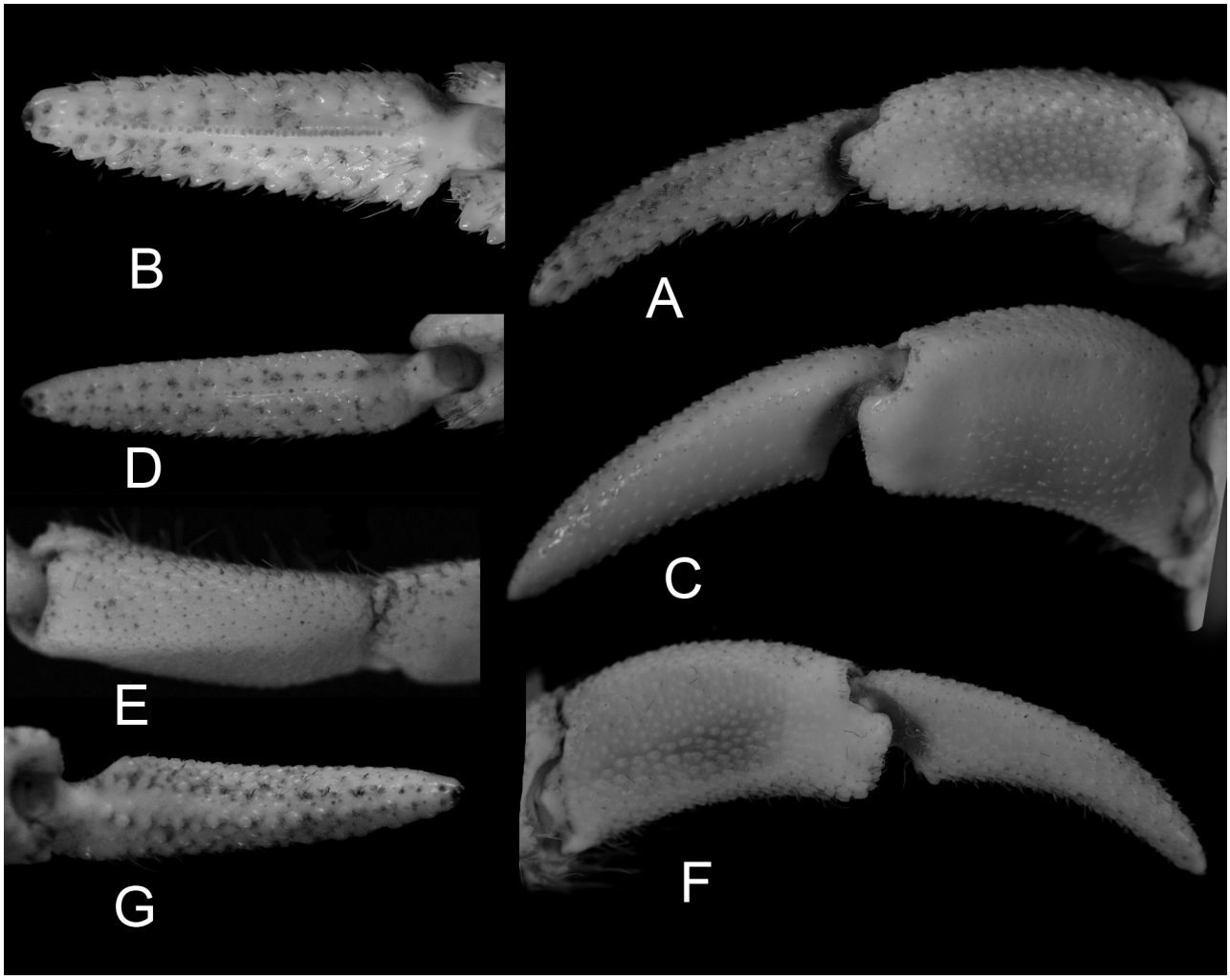

Fig. 3. *Coenobita moluccensis* n. sp. Holotype ♂ (SL 12.0 mm, MZB Cru 5722). A, dactylus and propodus of left P2, lateral view; B, dactylus of left P2, ventral view; C, dactylus and propodus of left P3, lateral view; D, dactylus of left P3, ventral view; E, propodus of left P3, dorsal view; F dactylus and propodus of right P3, lateral view; G, dactylus of right P3, ventral view.

scales. P5 chelate; chela and propodus with numerous corneous scales.

In male, coxae of P5 (Figs. 1D, 2D) thick, each forming moderately short, subtriangular, calcified sexual tube, left tube slightly broader and stouter than right. Gonopore positioned on small, triangular posterior projection or papillae, obscured by coarse, with dense setae; moderately large, subquadrangular sternal protuberance between both coxae.

Telson (Fig. 1E) with distinct lateral indentation, separating anterior and posterior lobes. Anterior lobe shorter than posterior lobe. Posterior lobe separated by narrow indentation; left lobe slightly broader and longer with posterior margin rounded, posterior margin of right lobe truncate; both margins with row of setae.

Variation: Morphological variation related to the size of specimen is observed in the degree of tuberculation or spination on the chelipeds and ambulatory legs. In specimens with SL < 12 mm, the tubercles are low and less dense on the palm of the chelipeds and on the ambulatory legs.

Color in life: Body and pereopods typically exhibiting base color with variations: cream, light orange, yellow-brown, darker brown. Chelipeds with upper surface of merus yellow or orange. P2 and P3 with orange, brown, or dark brown patches. Juveniles' body white or cream-colored; P2 and P3 sometimes weak orange or yellow (Fig. 4).

Size: Largest male SL 16.0 mm; largest female (ovig.) 6.7 mm.

Etymology: The specific name *moluccensis* is derived from Maluku (= Moluccas), referring to the type locality, Aru Island, in the Maluku Islands.

Ecological notes: According to local people on Aru Island, the habitat consists of white sandy beaches, and this species is sympatric with *C. brevimanus*, *C. rugosus*, and *C. violascens*.

Distribution: Indonesia (Aru Island, Maluku).

Remarks: See Remarks under *C. celebensis* n. sp.

***Coenobita patsyae* n. sp.**

(Figs. 5–8, 13C, D)

urn:lsid:zoobank.org:act:68E5DF8D-6A4D-4797-99E2-C75A5044E8E2

Material examined: Holotype: ♂ (15.0 mm) (MZB Cru 5725), Gulf of Tomini, Central Sulawesi, coll. local people, 2022. Paratypes: 2 ♂♂ (9.3, 10.1 mm) (MZB Cru 5726), 3 ♂♂ (7.7, 9.4, 11.1 mm) (ZRC 2023.0254), 4 ♂♂ (7.1, 8.4, 9.0, 9.7 mm) (NCHUZOOL 15278), 2 ♂♂ (9.7, 12.1 mm), 1 ♀ (5.7 mm) (NCHUZOOL 15280), same data as holotype. Others: 4 ♂♂ (7.7, 12.1, 15.5, 16.9 mm), 1 ♀ (9.8 mm) (NCHUZOOL 15271), Gulf of Tomini, Central Sulawesi, coll. local people, Dec. 2023; 3 ♂♂ (7.2, 10.1, 10.4 mm) (NCHUZOOL 15275), Central Sulawesi, coll. local people, Dec. 2023; 4 ♂♂ (11.6, 14.4, 14.5, 16.5 mm), 3 ♀♀ (8.7, 9.9, 13.0 mm), 1 ovig. ♀ (9.1 mm) (NCHUZOOL 15272), 1 ♂ (13.8 mm) (NCHUZOOL 15273), Muna Island, Southeast Sulawesi, coll. local people, Dec. 2023; 1 ♂ (17.3 mm) (NCHUZOOL 15274), Buton Island, Southeast Sulawesi, coll. local people, Dec. 2023.

Diagnosis: Shield (Figs. 5A, 8A–C) transversely convex, about 1.6 times as long as broad; dorsal surface covered with small and large flattened tubercles. Ocular peduncles reaching half length of fifth article of antennal peduncles; basal article of antennular peduncles 0.7 times as long as penultimate article (Fig. 5B); second article of antennal peduncle (Figs. 5C, 13C, D) slender, long, reaching half length of fourth peduncular article. Chelipeds (Fig. 6A, B) unequal, dissimilar; left distinctly larger than right; brush of setae on upper margin and proximal inner surface of palm of both chelipeds. Outer surface of left cheliped palm covered with tubercles, large and closely-spaced on upper half, smaller and fewer on lower half; lower margin with small tubercles; lower proximal part angled, forming rounded lobe-like projection, continued to slightly upright lower margin of fixed finger; fixed finger with moderately dense tubercles; right cheliped covered entirely with corneous-tipped tubercles each with short setae. P2 and P3 dissimilar; dorsal surfaces of dactylus and propodus of left P2 (Fig. 7A, B) broad, slightly flattened, lateral surface with flattened tubercles, ventral surface of dactylus broad, with scattered corneous tubercles, median longitudinal ridge consisting of row of tiny, widely-spaced, corneous teeth. Lateral surface of dactylus of left P3 (Fig. 7C) smooth or slightly punctate; delimited dorsally by row of small tubercles; ventral surface (Fig. 7D) slightly concave, median longitudinal ridge consisting of row of tiny corneous teeth; dorsolateral margin not delimited or weakly delimited by row of small tubercles; propodus slightly convex on lateral surface, covered with flattened small tubercles; dorsal surface (Fig. 7E) flattened, slightly broadened distally, covered with flattened tubercles; ventral surface slightly concave, with rows of large tubercles, some with tufts of setae. Carpus and merus covered with small and large tubercles, some with short setae. Dactyli and propodi of right P2 and P3 covered with tubercles on lateral surfaces; right P3 propodus lateral surface narrower than left P3 (Fig. 7F), ventral surface of dactylus with scattered small corneous spines (Fig. 7G). P4 semi-chelate (Fig. 6C). In male, coxae of P5 thick, each forming moderately short, calcified sexual tube; large, ovate sternal protuberance between

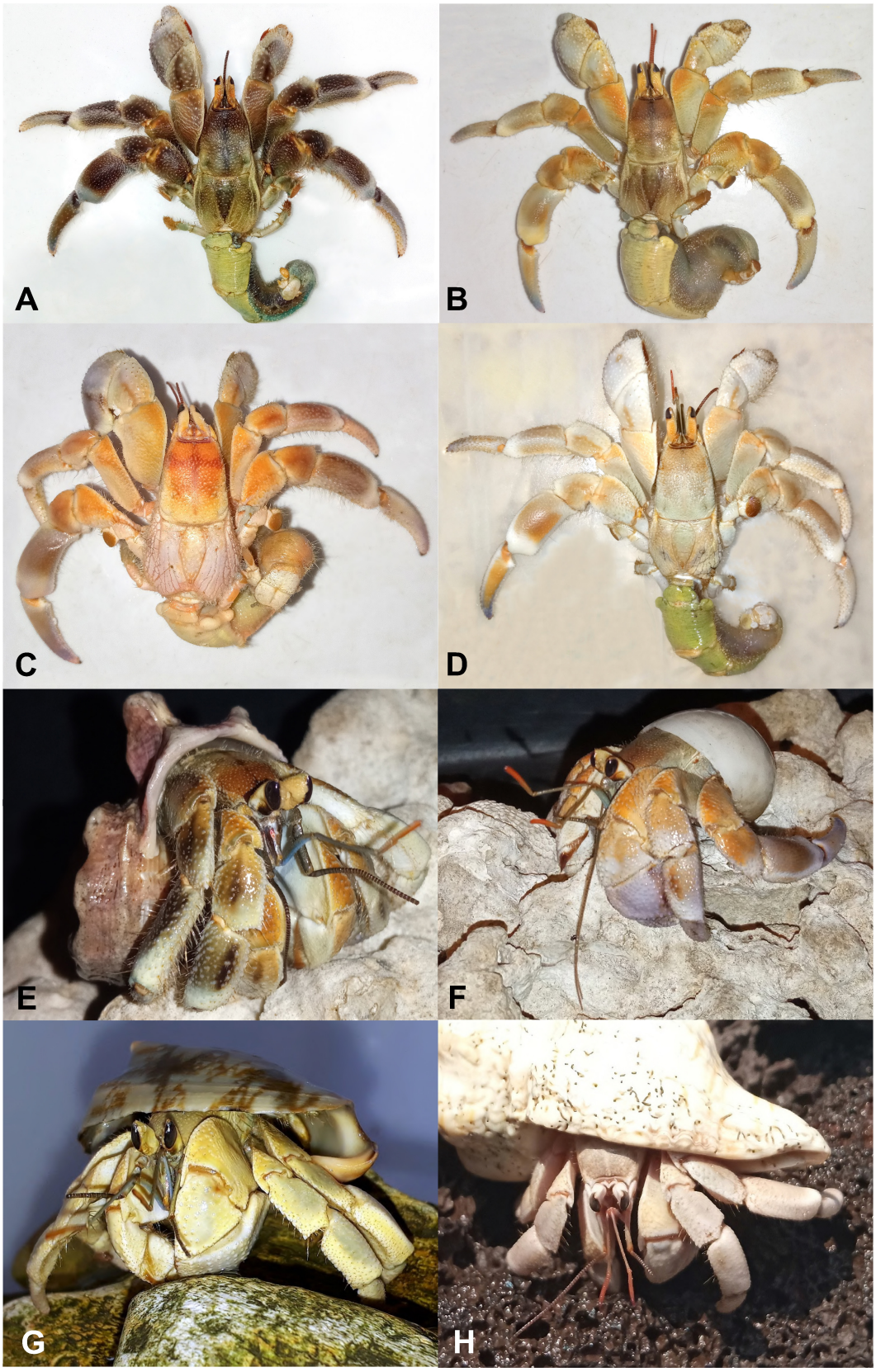

Fig. 4. Color in life of *Coenobita moluccensis* n. sp. A–D, tissue samples (see Table 1). A, TS COx100; B, TS COx105; C, TS COx104; D, TS COx94. All specimens from Aru Island, Maluku, Indonesia; not kept.

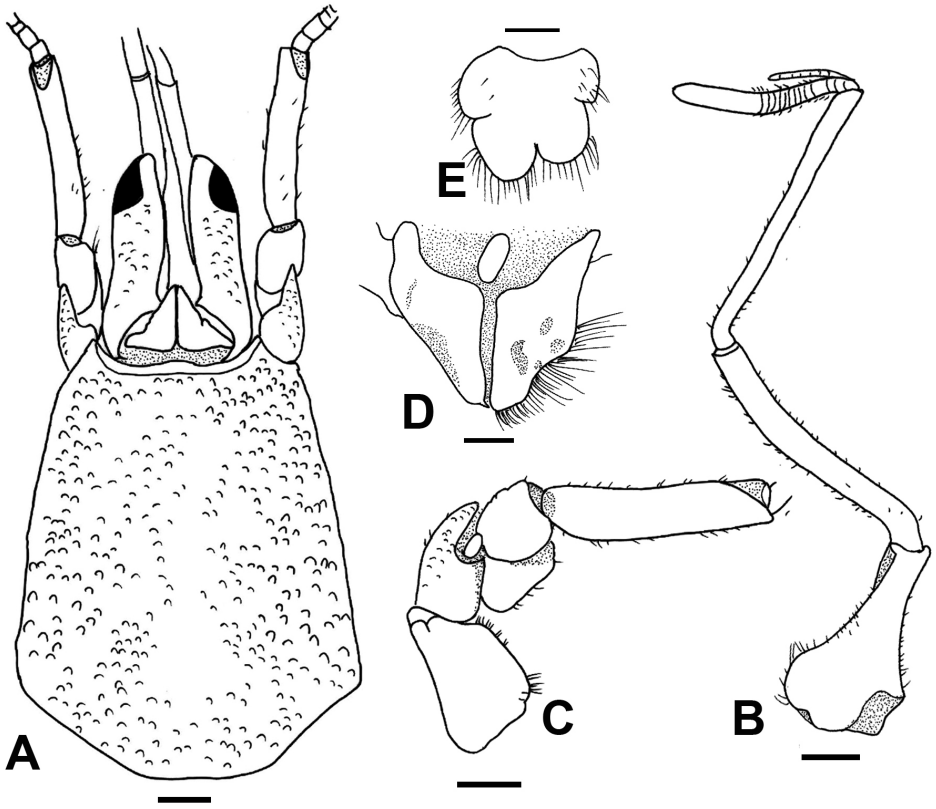

Fig. 5. *Coenobita patsyae* n. sp. Holotype ♂ (SL 15.0 mm, MZB Cru 5725). A, shield and cephalic appendages; B, right antennular peduncles, lateral view; C, right antennal peduncles, lateral view; D, sternite and coxae of male P5; E, telson. Setae partially omitted. Scale bars: A–E = 2 mm.

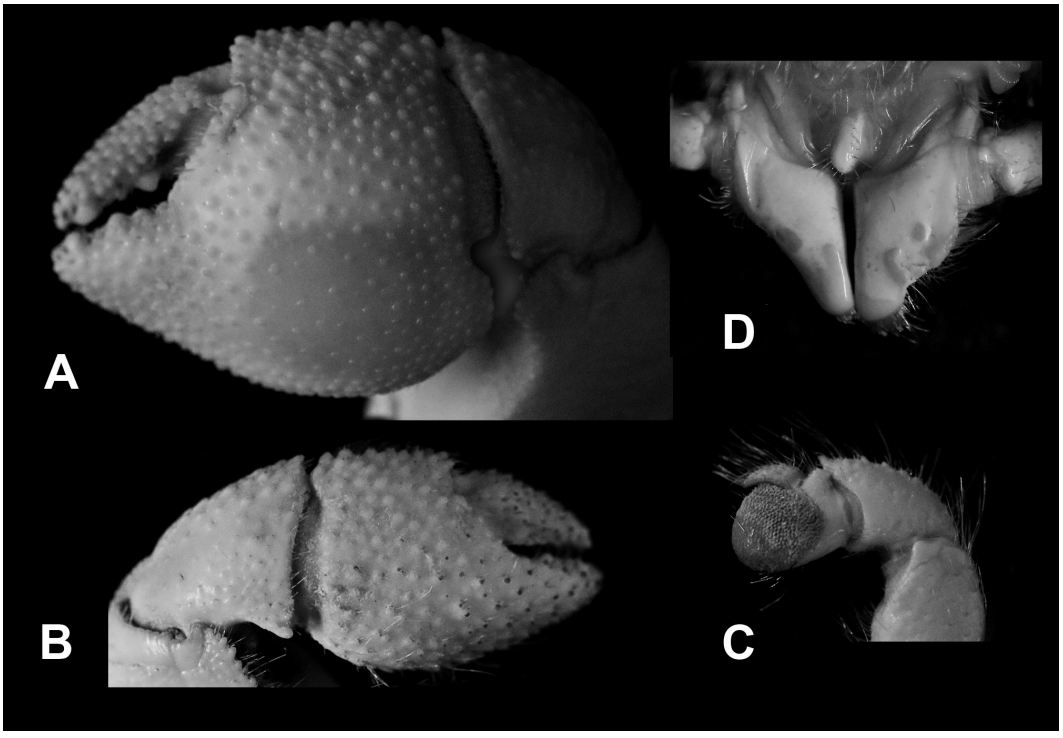

Fig. 6. *Coenobita patsyae* n. sp. Holotype ♂ (SL 15.0 mm, MZB Cru 5725). A, left cheliped, outer view; B, right cheliped, outer view; C, left P4, lateral view; D, sternite and coxae of male P5.

both coxae (Figs. 5D, 6D). Telson (Fig. 5E) posterior lobes subequal, margin rounded, left slightly longer, separated by deep and narrow median cleft from right lobe.

Variation: In some specimens (*e.g.*, the holotype), the dorsolateral margin of the left P3 propodus is not well-defined, while in others, it has a clearly delimited dorsolateral margin.

Color in life: Body and pereopods vary in color, including of dark brown, reddish-brown, and greenish-gray. Ocular peduncles may be white or pale yellow; merus of chelipeds typically showing varying degrees of yellow or orange, but may be absent in some individuals. P2 and P3 with black or dark brown patches. Juveniles' body white or cream-colored; P2 and P3 sometimes faintly orange or yellow (Fig. 8).

Size: Largest male SL 17.3 mm; largest female 13.0 mm.

Etymology: The specific name honors Patsy A. McLaughlin, in recognition of her significant contributions to the systematics of hermit crabs, including *Coenobita*.

Ecological notes: The habitat consists of beaches with low shrubs, sometimes bordered by

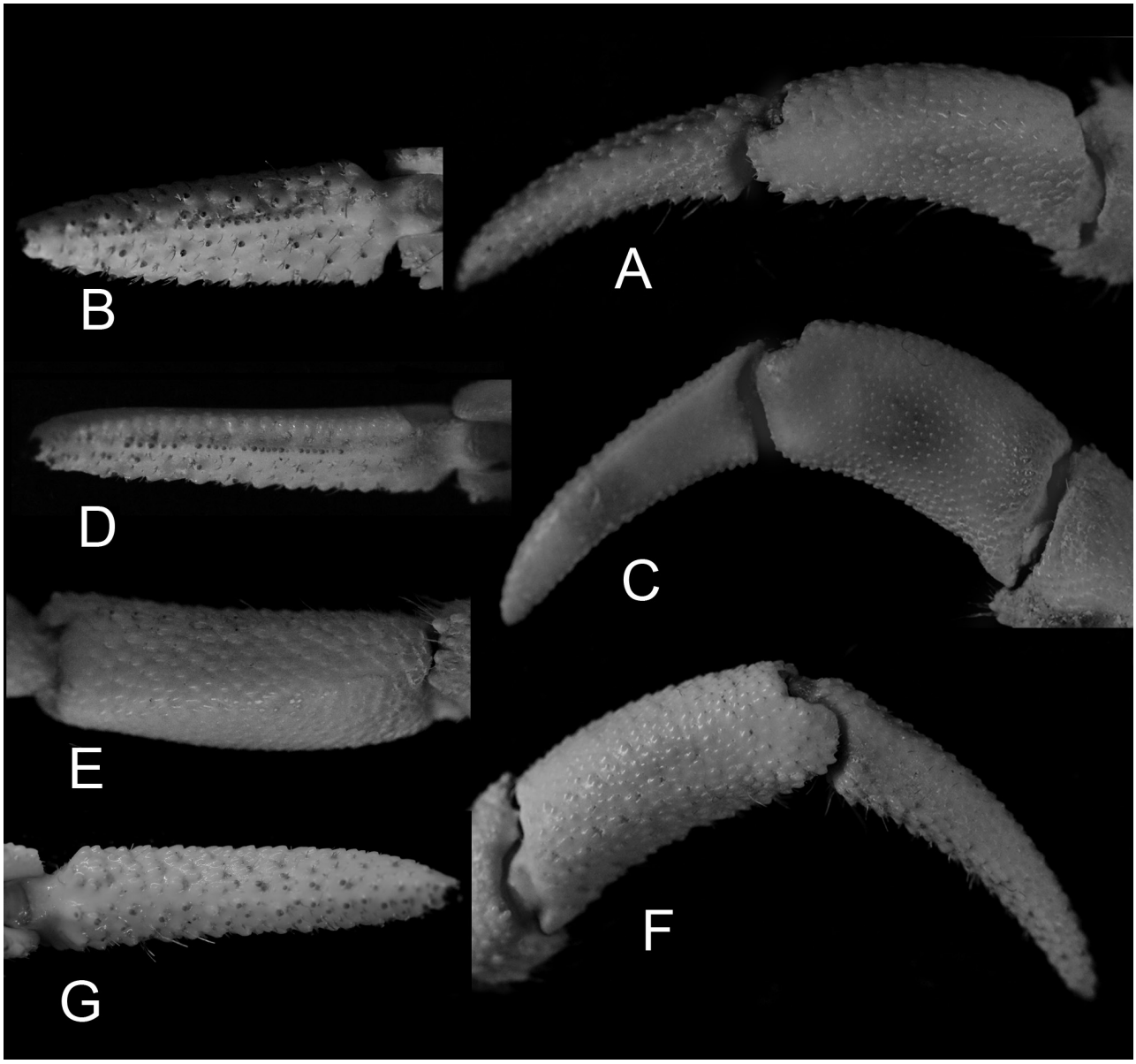

Fig. 7. *Coenobita patsyae* n. sp. Holotype ♂ (SL 15.0 mm, MZB Cru 5725). A, dactylus and propodus of left P2, lateral view; B, dactylus of left P2, ventral view; C, dactylus and propodus of left P3, lateral view; D, dactylus of left P3, ventral view; E, propodus of left P3, dorsal view; F dactylus and propodus of right P3, lateral view; G, dactylus of right P3, ventral view.

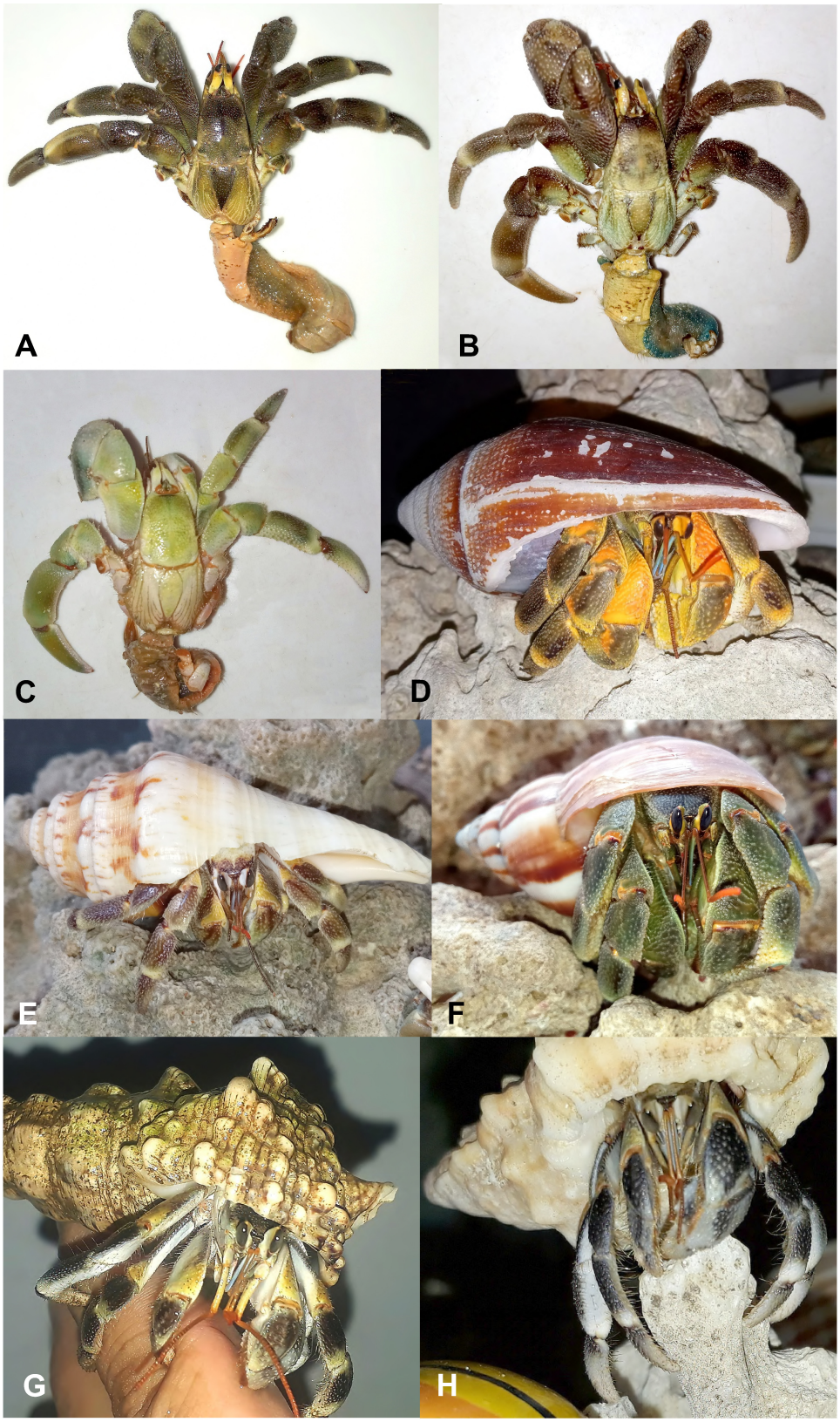

Fig. 8. Color in life of *Coenobita patsyae* n. sp. A, ♂ (SL 14.4 mm, NCHUZOOL 15272, Southeast Sulawesi); C, ♀ (SL 8.7 mm, NCHUZOOL 15272, Southeast Sulawesi); D, ♂ (SL 13.8 mm, NCHUZOOL 15273, Central Sulawesi, Indonesia). B, E–H, specimens from Sulawesi, Indonesia; not kept.

mangrove swamps. This species is sympatric with *C. pseudorugosus* (Table 1; Shih et al. 2023a), *C. rugosus*, and *C. violascens*.

Distribution: Indonesia (Central Sulawesi and Southeast Sulawesi).

Remarks: See Remarks under *C. celebensis* n. sp.

***Coenobita celebensis* n. sp.**

(Figs. 9–12, 13E, F)

urn:lsid:zoobank.org:act:890B35ED-04FF-4157-B47D-CE6676F8C12B

Material examined: Holotype: ♂ (18.3 mm) (MZB Cru 5727), Gulf of Tomini, Central Sulawesi, coll. local people, Dec. 2022. Paratypes: 2 ♂♂ (9.5, 13.6 mm) (MZB Cru 5728), 2 ♂♂ (11.7, 17.4 mm) (ZRC 2024.0263), 1 ♂ (11.1 mm) (NCHUZOOL 15279), 1 ♂ (16.8 mm) (NCHUZOOL 15281), 1 ♂ (11.7 mm) (NCHUZOOL 15277), same data as holotype. Others: Central Sulawesi, 1 ♂ (17.1 mm) (NCHUZOOL 15276), coll. local people, Dec. 2022.

Diagnosis: Shield (Figs. 9A, 12A, B) transversely convex, about 1.7 times as long as broad; dorsal surface covered with large flattened tubercles; basal article of antennular peduncle 0.8 times as long as penultimate article (Fig. 9B); second article of antennal peduncle (Figs. 9C, 13E, F) broad or stout, short, barely reaching base of fourth peduncular article, covered with small tubercles and sparse very short setae. Chelipeds (Fig. 10A, B) unequal, dissimilar; left distinctly larger than right; each with brush of setae on upper margin and proximal inner surface of palm. Outer surfaces of left cheliped dactylus and palm with rows of tubercles, large and closely-set on dactylus and upper half of palm, smaller on lower half; lower margin with strong tubercles; lower proximal part angled, forming oblique,

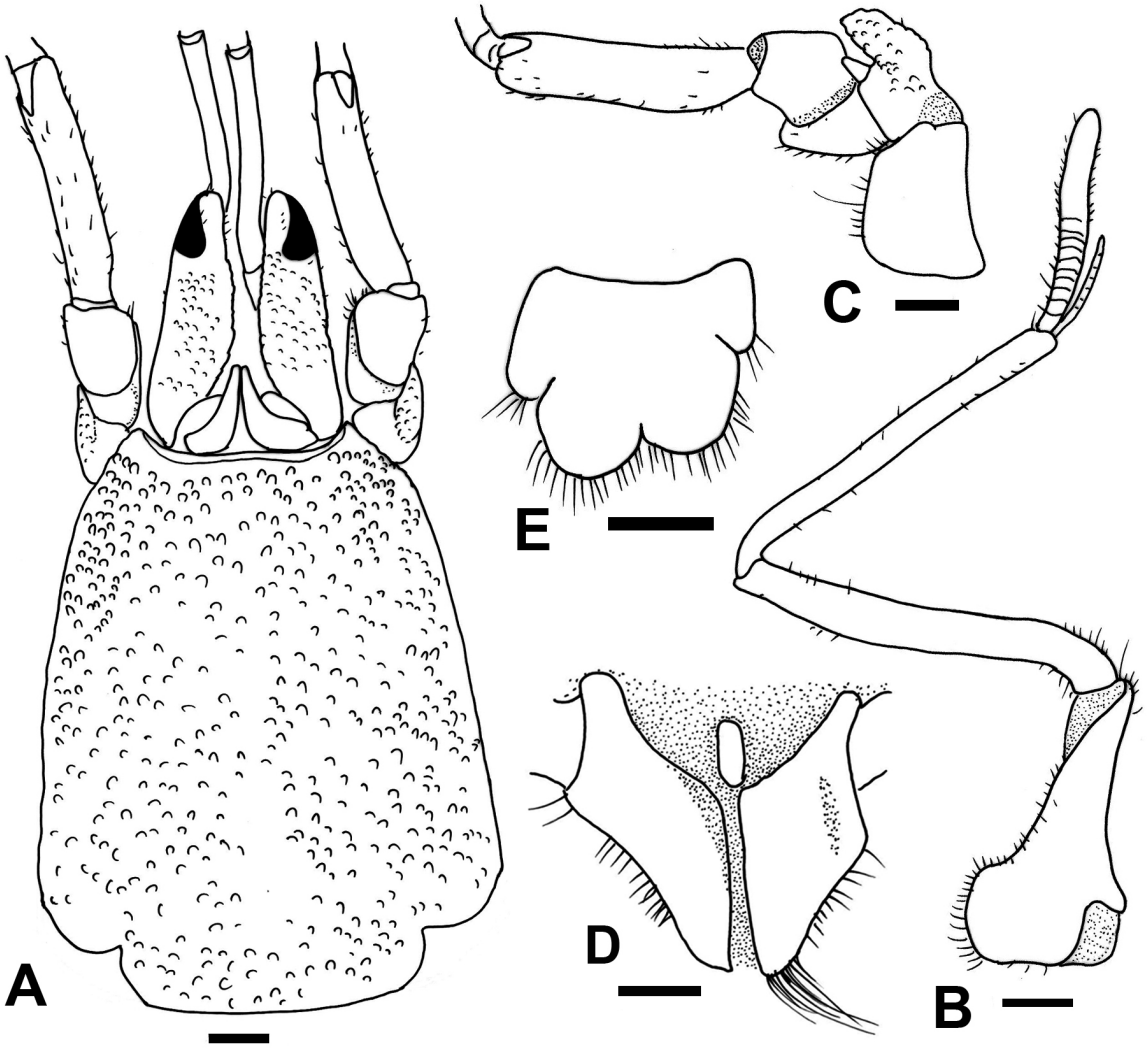

Fig. 9. *Coenobita celebensis* n. sp. Holotype ♂ (SL 18.3 mm, MZB Cru 5727). A, shield and cephalic appendages; B, right antennular peduncles, lateral view; C, right antennal peduncles, lateral view; D, sternite and coxae of male P5; E, telson. Setae partially omitted. Scale bars: A–E = 2 mm.

triangular, lobe-like projection, continued to slightly upright lower margin of fixed finger; outer surface of fixed finger with large tubercles. Right cheliped covered entirely with corneous-tipped tubercles each with short setae. P2 and P3 dissimilar, left stouter than right; P2 shorter, more slender than P3; dactylus and propodus of P2 (Fig. 11A, B) with corneous-tipped tubercles on lateral surfaces, dorsal surface broad, ventral surface of left P2 with median longitudinal ridge consisting of row of tiny corneous teeth; ventral surface of right P2 with irregular rows of corneous teeth. Left P3 (Fig. 11C) with lateral surface of dactylus punctate or with sparse tubercles; delimited dorsally by row of small tubercles; ventral surface (Fig. 11D) slightly concave, with median longitudinal ridge consisting of row of tiny corneous teeth; propodus convex on lateral surface, covered with transverse rows of small tubercles; dorsolateral margin delimited by row of small tubercles; dorsal surface (Fig. 11E) flattened, slightly broadened distally, covered with rows of flattened tubercles, each with very short setae, dorsomesial margin delimited by row of low tubercles, each with short setae. Right P3 (Fig. 11F, G) with dactylus covered with large tubercles, lateral surface of propodus with dense, transverse rows of large tubercles, ventral surface of dactylus with irregular rows of corneous-tipped tubercles. P4 semi-chelate (Fig. 10C). In male, coxae of P5 thick, each forming moderately short, subtriangular sexual tube; large, strongly produced, ovate sternal protuberance between both coxae (Figs. 9D, 10D). Telson (Fig. 9E) with posterior lobes asymmetrical, left slightly longer; lobes separated by narrow median cleft, margins with row of setae.

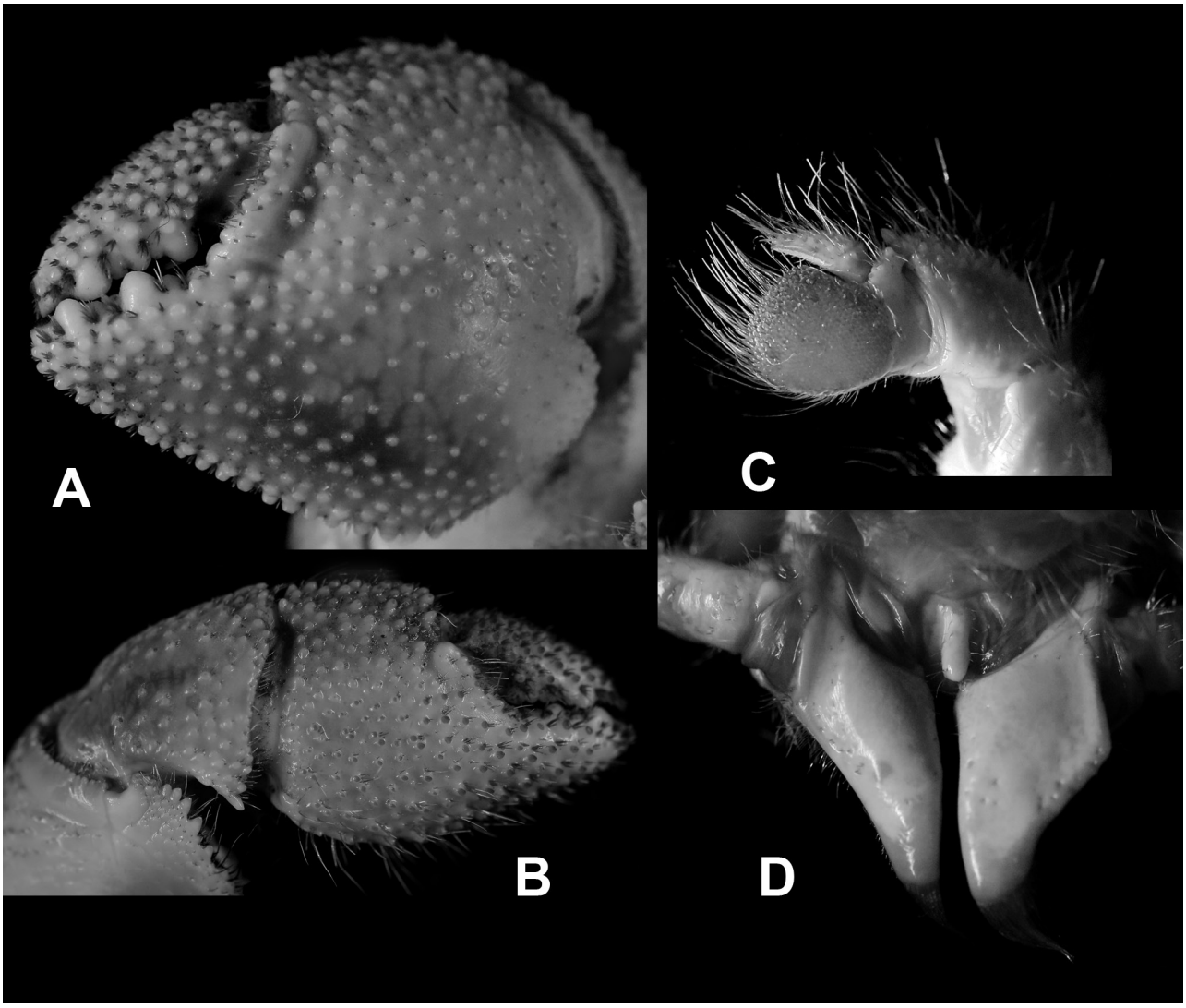

Fig. 10. *Coenobita celebensis* n. sp. Holotype ♂ (SL 18.3 mm, MZB Cru 5727). A, left cheliped, outer view; B, right cheliped, outer view; C, left P4, lateral view; D, sternite and coxae of male P5.

Color in life (Fig. 12): Usually dark brown in adults. Surface of shield with patch of black, dark brown or light brown anteriorly, transverse dark brown line distally; sometimes broad longitudinal dark brown stripe medially, orangish yellow line posteriorly. Ocular peduncles orangish brown or light brown mesially; cornea black or dark brown. Antennal peduncles greenish brown, flagella orange, antennular peduncles orange. Chelipeds with merus bright yellow or orange. P2 and P3 with merus partially yellow or orange; each segment having black or dark brown patches.

Size: Largest male SL 18.3 mm.

Etymology: The specific name *celebensis* is derived from Celebes (= Sulawesi), where all specimens were collected and are distributed to date.

Ecological notes: In Central Sulawesi, the habitat consists of sandy beaches bordered by rice fields and some creeks. This species is occasionally sympatric with *C. violascens*.

Distribution: Indonesia (Central Sulawesi).

Remarks: *Coenobita moluccensis* n. sp., *C. patsyae* n. sp., and *C. celebensis* n. sp. are very similar, sharing the following characters: palms of chelipeds covered with large and small tubercles; upper margin with brush of setae; no stridulatory ridge on the left cheliped palm, moderately short, triangular, stout male sexual tube on the coxae of P5; and yellow tinges on parts of the chelipeds and pereopods.

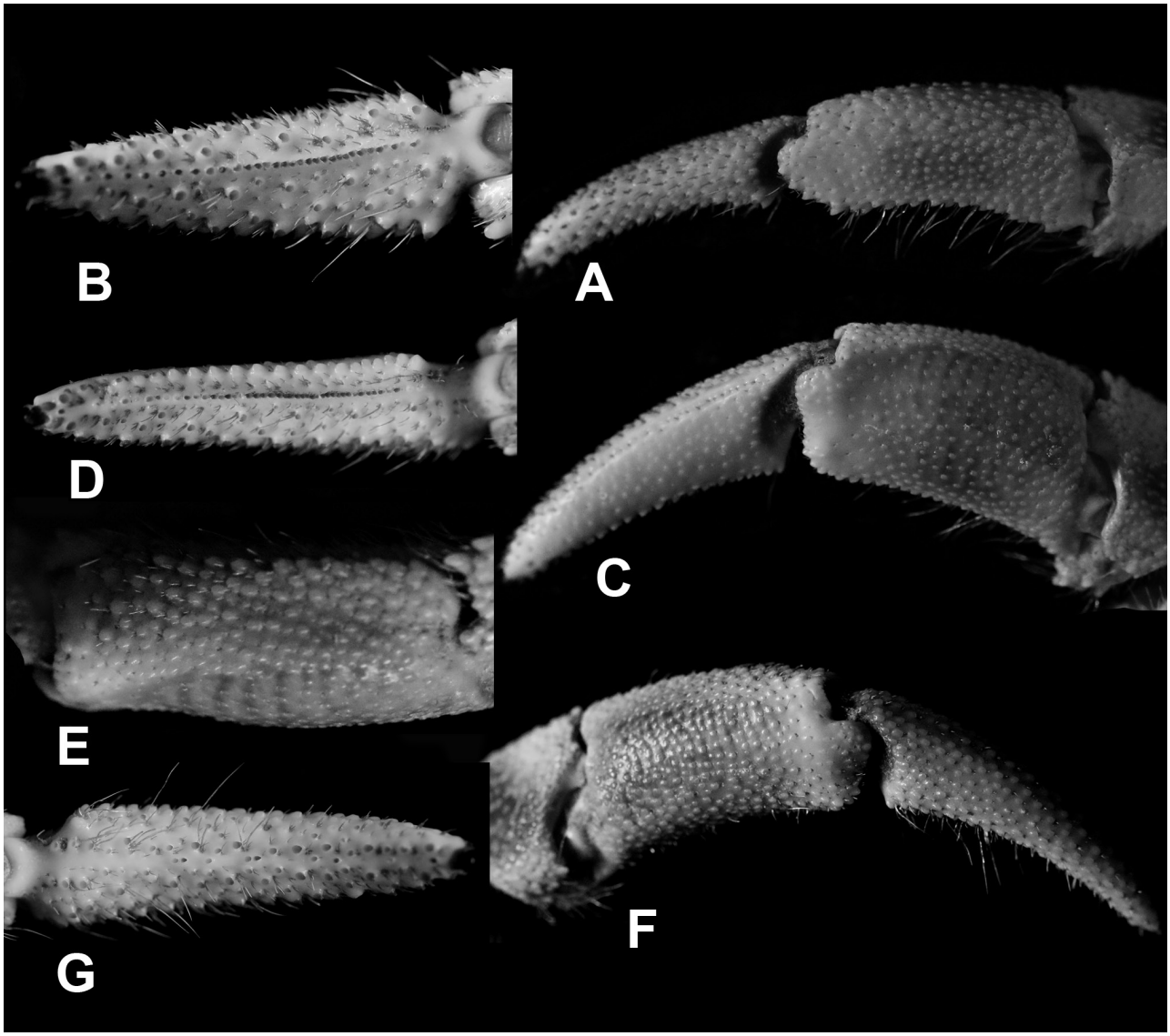

Fig. 11. *Coenobita celebensis* n. sp. Holotype ♂ (SL 18.3 mm, MZB Cru 5727). A, dactylus and propodus of left P2, lateral view; B, dactylus of left P2, ventral view; C, dactylus and propodus of left P3, lateral view; D, dactylus of left P3, ventral view; E, propodus of left P3, dorsal view; F dactylus and propodus of right P3, lateral view; G, dactylus of right P3, ventral view.

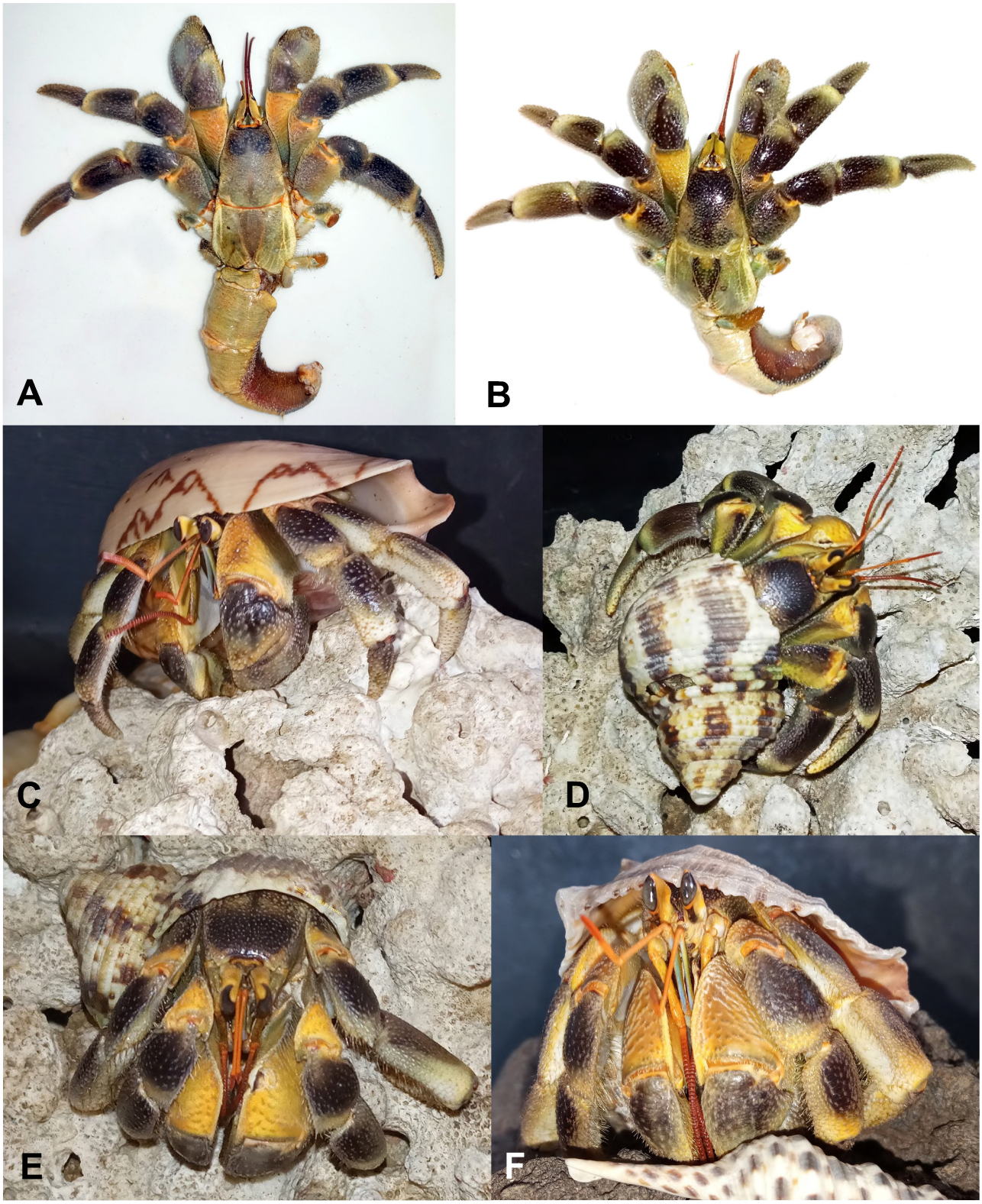

Fig. 12. Color in life of *Coenobita celebensis* n. sp. C, paratype ♂ (SL 15.5 mm, NCHUZOOL 15277, Central Sulawesi, Indonesia). A, B, D–F, specimens from Sulawesi, Indonesia; not kept.

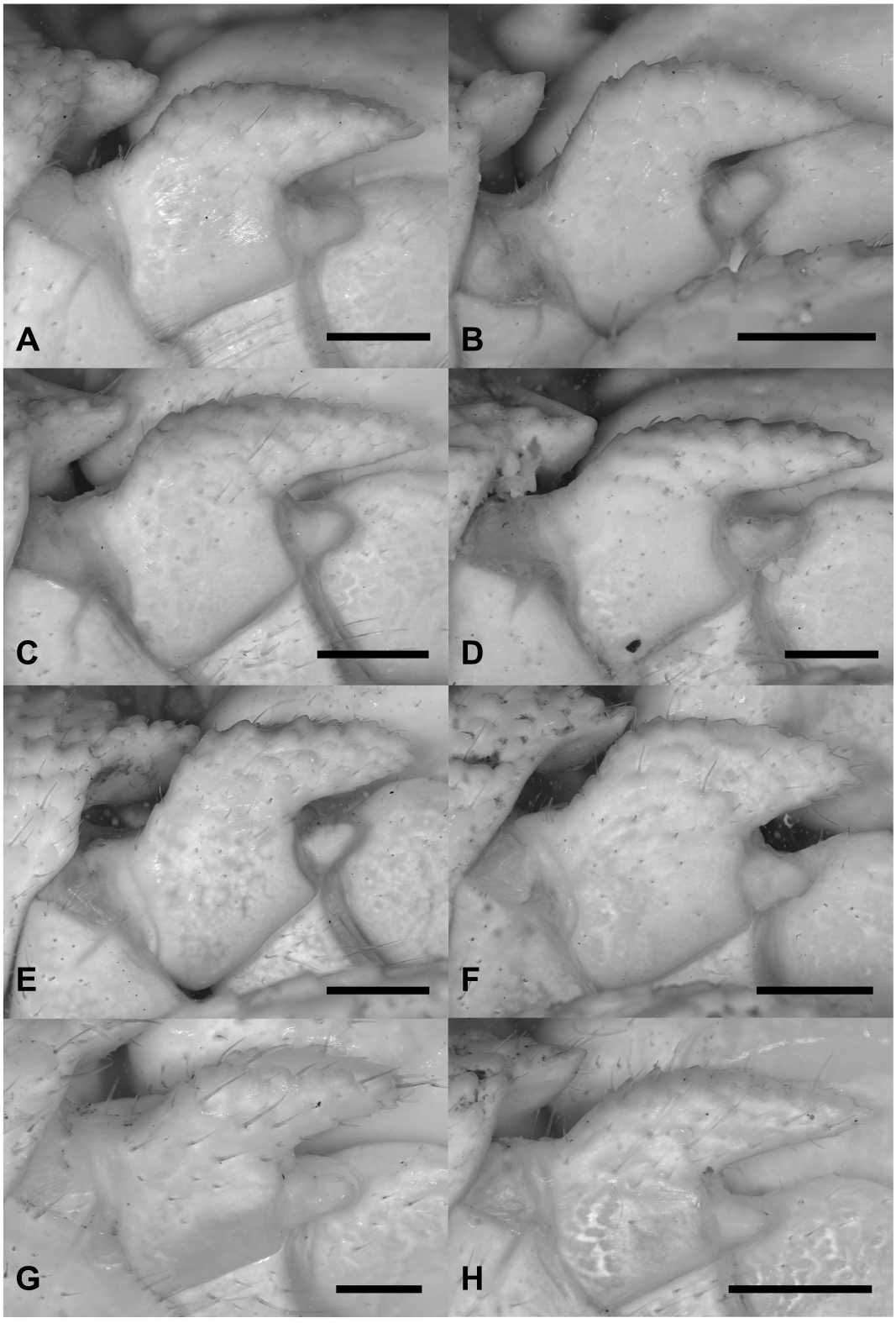

Fig. 13. Outer surface of the second article of the right antennal peduncles in *Coenobita moluccensis* n. sp. (A, B), *C. patsyae* n. sp. (C, D), *C. celebensis* n. sp. (E, F), and *C. lila* Rahayu, Shih & Ng, 2016 (G, H.). A, holotype ♂ (SL 12.0 mm; MZB Cru 5722); B, paratype ♂ (SL 14.4 mm; NCHUZOOL 15259); C, holotype ♂ (SL 15.0 mm; MZB Cru 5725); D, ♂ (SL 13.8 mm; NCHUZOOL 15273); E, holotype ♂ (SL 18.3 mm, MZB Cru 5727); F, paratype ♂ (SL 15.5 mm, NCHUZOOL 15277); G, paratype ♂ (SL 10.7 mm, NCHUZOOL 13624); H, ♂ (SL 11.3 mm NCHUZOOL 15284). Scale bars = 1 mm.

These three new species can be distinguished by the following characters (Table 2): 1) morphology of left P3 propodus: in *C. moluccensis*, dorsolateral margin delimited by row of small tubercles, with basal lateral surface slightly convex; surfaces punctate in most specimens (Fig. 3C); in *C. patsyae*, dorsolateral margin not delimited or weakly delimited by row of small tubercles, with basal lateral surface slightly convex; surfaces covered with small tubercles in most specimens (Fig. 7C); and in *C. celebensis*, dorsolateral margin delimited by row of small tubercles, with basal lateral surface convex; surfaces covered with large tubercles in most specimens (Fig. 11C); 2) shape of second article of antennal peduncles: stout (ratio of length from tip to inner base along middle/width from dorsal margin to inner base about 1.4) and short (not reaching proximal area of fourth article) in *C. moluccensis* (Figs. 1C, 13A, B); slender (ratio about 1.7) and long (reaching half length of fourth article) in *C. patsyae* (Figs. 5C, 13C, D); and broad or stout (ratio about 1–1.4) and short (barely reaching proximal area of fourth article) in *C. celebensis* (Figs. 9C, 13E, F); and 3) shape of sternal protuberance between male fifth coxae: large, subquadrangular in *C. moluccensis* (Figs. 1D, 2D); strongly produced, ovate in *C. patsyae* (Figs. 5D, 6D); strongly produced, long, ovate, in *C. celebensis* (Figs. 9D, 10D).

Fize and Serène (1955) stated that color alone is unreliable for distinguishing species within the genus *Coenobita*. However, the varying degree of yellow or orange, especially on the cheliped merus, can still be useful for differentiating most individuals of the three species from other congeners, particularly in larger individuals. In *C. moluccensis*, there is only a yellow or orange tinge (Fig. 4); in *C. patsyae*, the color ranges from yellow or orange to a yellow or orange tinge, with some individuals showing no yellow or orange tint (Fig. 8); and in *C. celebensis*, the color is consistently yellow or orange (Fig. 12).

The three new species are similar to *C. lila* and *C. cavipes* Stimpson, 1858 in which the left cheliped palm is covered by tubercles, without stridulatory ridge on the dorsal surface of the palm, with row of dense, stiff setae on dorsal surface of palm, and stout and subtriangular sexual tubes (*e.g.*, ca. 1.5–1.6 times as long as broad measured on mesial margin of right tube), but show differences as follows: 1) left P3 propodus broader, 1.6 times as long as broad in *C. moluccensis*, 1.8 times in *C. patsyae* and *C. celebensis* (1.9 times in *C. lila* and 2.3

Table 2. Comparison of characters and fresh colorations of *Coenobita moluccensis* n. sp., *C. patsyae* n. sp., *C. celebensis* n. sp., *C. lila* Rahayu, Shih & Ng, 2016, and *C. cavipes* Stimpson, 1858

Characters	*C. moluccensis*	*C. patsyae*	*C. celebensis*	*C. lila*	*C. cavipes*
Antennal peduncles	Second article stout, short, not reaching proximal area of fourth article (Figs. 1C, 13A, B).	Second article slender, long, reaching half length of fourth article (Figs. 5C, 13C, D).	Second article stout or broad, short, barely reaching proximal area of fourth article (Figs. 9C, 13E, F).	Second article stout, short, not reaching proximal area of fourth article (Rahayu et al. 2016: fig. 1C; Fig. 13G, H).	Second article slender, long, reaching half length of fourth article (Rahayu et al. 2016: fig. 7C).
Propodus of left P3	Broader (1.6 times as long as broad); dorsolateral margin delimited by row of small tubercles, basal lateral surface slightly convex; surfaces punctate (Fig. 3C).	Slightly broader (1.8 times as long as broad); dorsolateral margin not delimited or weakly delimited by row of small tubercles, basal lateral surface slightly convex; surfaces covered with small tubercles (Fig. 7C).	Slightly broader (1.8 times as long as broad); dorsolateral margin delimited by row of small tubercles, basal lateral surface convex; surfaces covered with large tubercles (Fig. 11C).	Sightly narrower (1.9 times as long as broad); dorsolateral margin delimited only on 4/5 by weak tubercles, basal lateral surface slightly convex; surfaces covered with corneous-tipped tubercles (Rahayu et al. 2016: figs. 2E, 5A–C, 6A–C).	Narrower (2.3 times as long as broad); dorsolateral margin delimited by row of corneous-tipped tubercles, , basal lateral surface slightly convex; surfaces only with few scattered tubercles (Rahayu et al. 2016: figs. 5D–F, 6D–F, 8E).
Coxae of P5	Sternal protuberance large, subquadrate (Figs. 1D, 2D).	Sternal protuberance moderately large, ovate, produced (Figs. 5D, 6D).	Sternal protuberance large, ovate, strongly produced (Figs. 9D, 10D).	Sternal protuberance large, subpentagonal (Rahayu et al. 2016: figs. 1D, 2G).	Sternal protuberance moderately large, cylindrical (Rahayu et al. 2016: figs. 7D, 8G).
Color on cheliped merus	Only a yellow or orange tinge (Fig. 4).	Ranges from yellow or orange to a yellow or orange tinge, with some individuals showing no yellow or orange tint (Fig. 8).	Consistently yellow or orange (Fig. 12).	No yellow or orange tinge; some with very faint tinge (Rahayu et al. 2016: figs. 10, 11A–C).	Consistently brown or greenish brown (Rahayu et al. 2016: fig. 11D–F).

times in *C. cavipes*) (Table 2); 2) sternal protuberance subquadrangular in *C. moluccensis*; produced and ovate in *C. patsyae*; and strongly produced, ovate and long in *C. celebensis* (subpentagonal in *C. lila* and cylindrical in *C. cavipes*) (Table 2); and 3) dactyli of right P2 and P3 with scattered corneous spines on ventral surface in the three new species and *C. lila*, but a row of tiny corneous teeth medially in *C. cavipes*.

***Coenobita granularis* n. sp.**

(Figs. 14–17)

urn:lsid:zoobank.org:act:A21F7F9F-761E-4072-AF49-E1A49EE23A0B

Material examined: Holotype: ♂ (10.4 mm) (MZB Cru 5729), Gulf of Tomini, Central Sulawesi, Indonesia, coll. local people, 2022. Paratypes: 1 ♂ (8.7 mm), 1 ♀ (10.9 mm) (MZB Cru 5730), 2 ♂♂ (10, 10.8 mm) (ZRC 2024.0263), 1 ♂ (10.7 mm), 1 ♀ (8.0 mm) (NCHUZOOL 15255), same data as holotype. Others: 4 ♂♂ (7.6, 8.7, 9.2, 11.5 mm), 1 ♀ (7.7 mm) (MZB Cru 5791), 4 ♂♂ (7.3, 8.3, 8.9, 11.1 mm), 1 ♀ (7.4 mm) (ZRC 2023.0253), 3 ♂♂ (8.7, 8.8, 9.0 mm) (NCHUZOOL 15254), 4 ♂♂ (8.2, 9.1, 9.6, 9.8 mm), 2 ♀♀ (8.5, 9.0 mm) (NCHUZOOL 15256), same data as holotype.

Diagnosis: Shield (Figs. 14A, 17A–C), transversely convex, about 1.5 times as long as broad; dorsal surface punctate, tubercles on dorsodistal surface. Ocular peduncles reaching third proximal of ultimate article of antennal peduncles, basal article of antennular peduncles 0.6 times as long as penultimate article (Fig. 14B); antennal peduncles (Fig. 14C) exceeding ocular peduncles by half length of fifth article, second article slender, smooth. Chelipeds (Fig. 15A, B) unequal and dissimilar, left larger than right, brush of setae on half proximal of upper margin of both palms; left cheliped palm with row of 5–6 stridulatory apparatus (laminar ridge) on upper outer surface, outer surface with widely-spaced tubercles, sometimes corneous-tipped; lower margin of palm oblique, with corneous-tipped tubercles bearing tufts of short setae; lower proximal angled rounded or 3 cornered. P2 and P3 dissimilar (Fig. 16), P2 markedly more slender than P3. Lateral surfaces of dactylus and propodus of left P2 (Fig. 16A) with numerous flattened tubercles bearing tufts of short setae, ventral surface of dactylus (Fig. 16B) with longitudinal ridge consisting of row of tiny corneous teeth, closely-spaced proximally, widely-spaced distally. Right P2 slightly shorter, armament similar. Lateral surface of dactylus and propodus of left P3 (Fig. 16C–E) broad, punctate; ventral surface of dactylus (Fig. 16D) slightly concave, median longitudinal ridge consisting of row of tiny corneous teeth. Right P3 slightly more slender than left. Dactylus and propodus (Fig. 16F) covered with flattened tubercles; ventral surface of dactylus (Fig. 16G) with sparse, low corneous-tip tubercles. P4 semi-chelate (Fig. 15C). In male, coxae of P5 thick, each forming calcified sexual tube, right tube long, directed to left, left tube short, broader than right; gonopore positioned on moderately broad with truncate tip posterior projection or papillae, with short, sparse, setae; cylindrical, small, sternal protuberance between both coxae (Figs. 14D, F, 15D, E). Telson (Fig. 14E) posterior lobes slightly asymmetrical separated by narrow median cleft; margins rounded, with row of setae.

Description: Shield (Figs. 14A, 17A–C) transversely convex, about 1.5 times as long as broad; anterior margin between rostrum and lateral projections slightly concave; lateral projection produced, terminating in pointed spine; posterior margin slightly convex. Rostrum broadly rounded, obsolete. Lateral surface smooth, with numerous tufts of long setae; dorsal surface punctate, tubercles on dorsodistal surface.

Ocular peduncles (Fig. 14A) concave laterally, mesial surface compressed, reaching third proximal of ultimate segment of antennal peduncles; cornea small, occupying slightly more than half of distal part of ocular peduncles laterally; dorsal surface punctate with short setae. Ocular acicles triangular, terminating acutely.

Antennular peduncles (Fig. 14B) long. Basal segment 0.6 times as long as penultimate segment. Ultimate segment 1.1 times as long as penultimate segment. Upper rami of flagella stick-like, terminating in rounded tip, with very short setae on lateral and mesial margins.

Antennal peduncles (Fig. 14C) exceeding ocular peduncles by half length of fifth segment, reaching third proximal of penultimate segment of antennular peduncles. First segment 1.4 times as long as broad. Second segment slender, smooth. Third, fourth and fifth segments unarmed, with scattered, very short setae. Antennal acicle short, fused to second segment of peduncle. Flagella long, far exceeding tip of left cheliped.

Chelipeds (Fig. 15A, B) unequal and dissimilar, left larger than right. Dactylus of left cheliped (Fig. 15A) with numerous broad, flattened tubercles bearing short setae on outer surface, upper margin with row of corneous-tipped spines and short, stiff setae; inner surface with rows of corneous-tipped tubercles bearing short setae; cutting edge with 3 large teeth terminating in small corneous claw. Row of 5–6 stridulatory apparatus (laminar ridge) on upper outer surface of palm. Outer surface of fixed finger with few tubercles, some with corneous-tipped; lower margin straight with row of large tubercles, some with corneous-tipped, each

bearing tufts of short setae; inner surface with few of corneous tipped tubercles; cutting edge with 2 large and 2 small teeth, terminating in small corneous claw. Palm with upper margin bearing row of corneous spines and brush of long, coarse setae, outer surface with widely-spaced tubercles, sometimes corneous-tipped; lower margin oblique, with corneous-tipped tubercles bearing tufts of short setae; lower proximal angled rounded or 3 cornered; inner surface with punctate with short setae, longitudinal ridge consisted of large tubercle starting at base of cutting edge to articulation with carpus, larger tubercles adjacent to ridge; brush of setae proximally near upper margin. Carpus with tubercles with tufts of short setae arranged more or less in longitudinal rows on outer surface near upper margin, narrow, smooth area medially, less dense, flattened tubercles near lower margin; inner surface with few small, flattened tubercles bearing short tufts of setae. Merus with transverse rows of flattened tubercles bearing very short setae on outer surface; lower margin produced distally, lower inner margin almost smooth but with tufts of long setae; inner and lower surfaces smooth but with few transverse tufts of very short setae.

Right cheliped (Fig. 15B) with upper margin of dactylus bearing row of corneous-tipped tubercles, outer surface with widely-spaced flattened tubercles and short setae; palm with row of corneous spines and thick brush of long coarse setae on upper margin; cutting edges of

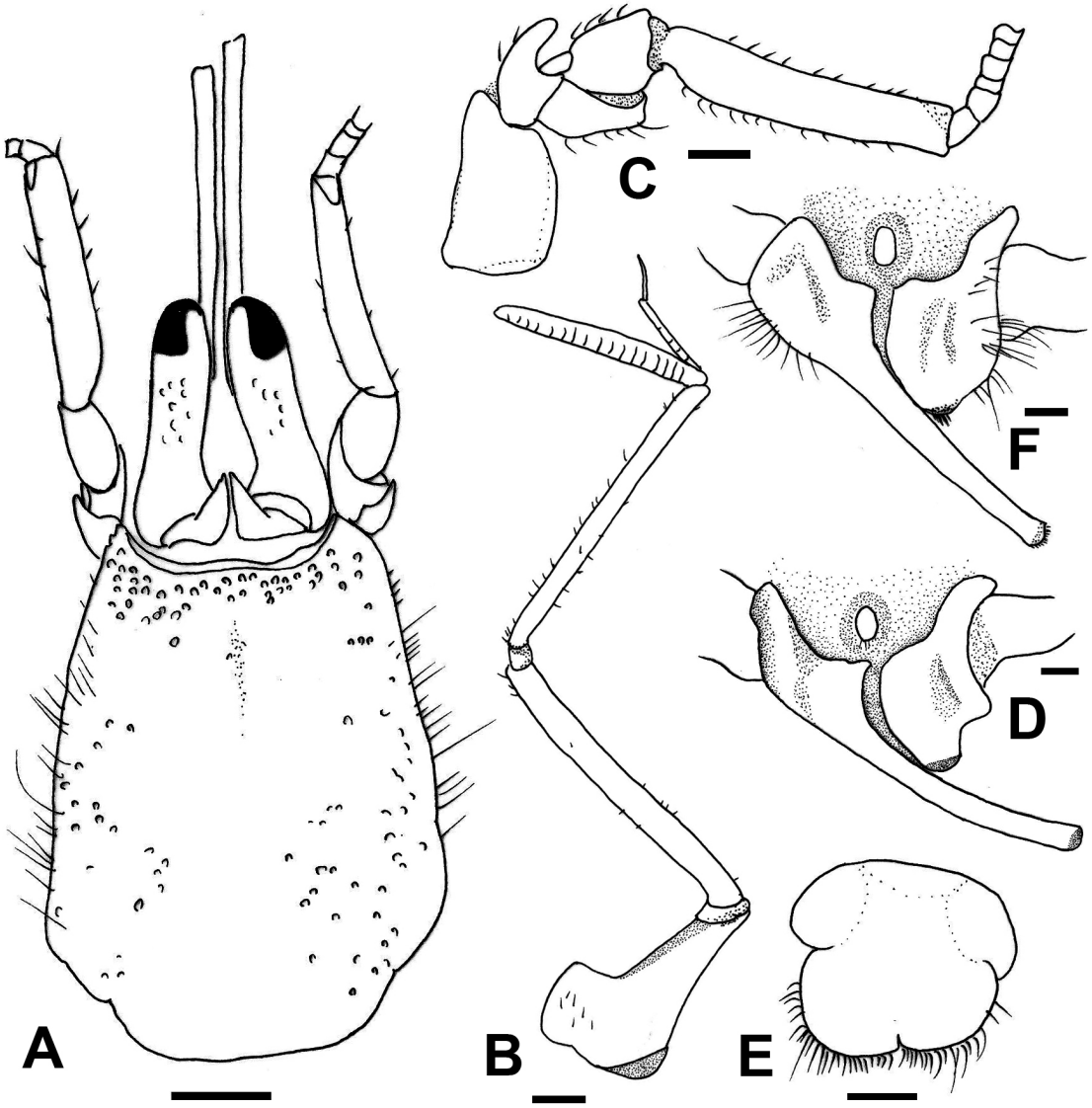

Fig. 14. *Coenobita granularis* n. sp. A–E, holotype ♂ (SL 10.4 mm, MZB Cru 5729); F, paratype ♂ (SL 10.7 mm, NCHUZOOL 15255). A, shield and cephalic appendages; B, right antennular peduncles, lateral view; C, right antennal peduncles, lateral view; D, F, sternite and coxae of male P5; E, telson. Setae partially omitted. Scale bars: A = 2 mm; B–E = 1 mm.

dactylus and fixed finger each with large tooth adjacent to corneous claw, followed by row of small teeth. Outer surfaces of palm and fixed finger compressed, with rows of flattened, corneous-tipped tubercles, each bearing short setae, lower margin with row of long, stiff setae; inner surfaces of palm and dactylus with scattered corneous-tipped tubercles, each with tufts of setae; proximal area of palm with long, coarse setae near upper margin. Carpus and merus compressed laterally, similarly armed as left cheliped.

P2 and P3 dissimilar (Fig. 16A, C, F), P2 markedly more slender than P3. Dactylus of left P2 with rows of corneous-tipped tubercles each with short setae on lateral surface; dorsal surface flattened, not delimited, with widely-spaced rows of corneous-tipped tubercles; mesial surface with rows of widely-spaced flattened, corneous-tipped tubercles each bearing tufts of short setae; ventral surface (Fig. 16B) with longitudinal ridge consisting of row of tiny corneous teeth, closely-spaced proximally, widely-spaced distally, ventrolateral margin with row of corneous-tipped tubercles bearing tufts of setae. Propodus broad dorsal surface with rows of low tubercles, some with corneous-tipped, dorsomesial margin with row of corneous-tipped tubercles, dorsolateral surface not delimited, lateral surface compressed, with numerous flattened tubercles bearing tufts of short setae; ventrolateral surface with row of corneous-tipped tubercles and rather long setae, mesial surface concave, transverse row of flattened tubercles each with short setae. Carpus with row of small tubercles each bearing short setae on dorsolateral margin, lateral surface with row of flattened tubercles each bearing tufts of setae; mesial surface compressed, with few tufts of short setae. Merus compressed laterally

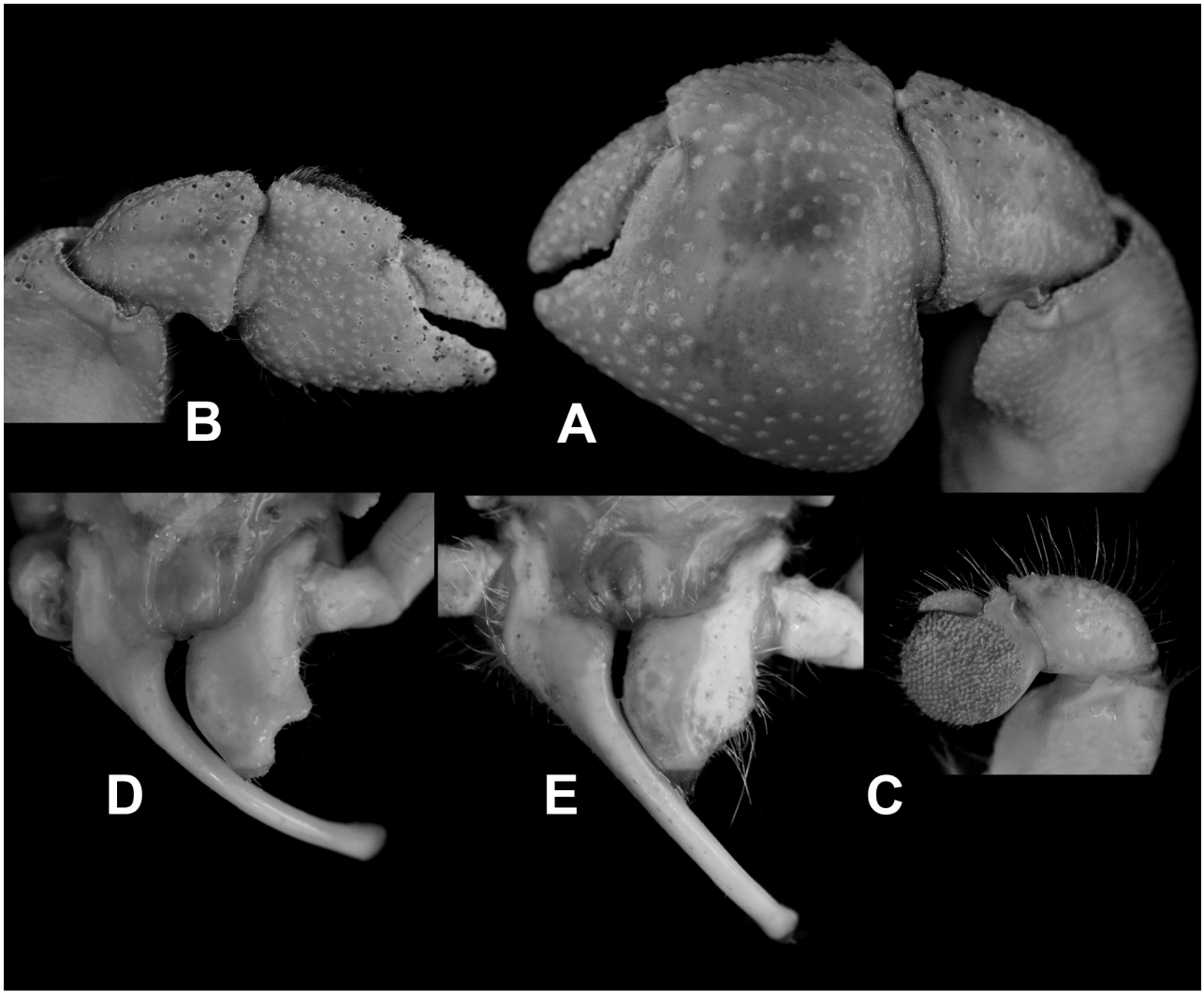

Fig. 15. *Coenobita granularis* n. sp. A–D, holotype ♂ (SL 10.4 mm, MZB Cru 5729); E, paratype ♂ (SL 10.7 mm, NCHUZOOL 15255). A, left cheliped, outer view; B, right cheliped, outer view; C, left P4, lateral view; D, E, sternite and coxae of male P5.

and mesially, with tufts of long setae on dorsal and ventral margins, transverse row of transverse tufts of setae on lateral surface; mesial surface almost smooth, ventral margin with row of moderately large tubercles. Right P2 slightly shorter than left. Armament similar.

Left P3 with dactylus slightly shorter than or same length as propodus (Fig. 16C), lateral surface slightly convex distally, flattened proximally, punctate, delimited dorsally by row of tubercles bearing short setae, dorsal surface with longitudinal rows of corneous-tipped tubercles each with tufts of setae, decreasing in size proximally; mesial surface with rows of corneous-tipped tubercles each with tufts of setae; ventrolateral margin with row of widely-spaced corneous small spines with short setae; ventral surface (Fig. 16D) slightly concave, median longitudinal ridge consisting of row of tiny corneous teeth, not reaching tip. Propodus slightly flattened distally on lateral surface, becoming convex proximally, punctate; dorsolateral margin not delimited by row of tubercles; dorsal surface (Fig. 16E) flattened, distally broad, slightly narrower proximally, with rows of flattened tubercles; dorsomesial margin delimited by row of tubercles sometimes with corneous-tipped and short setae; mesial surface slightly concave, with transverse rows of tufts of setae; ventral surface slightly concave with widely-spaced tubercles and scattered tufts of setae; ventrolateral margin with row of tubercles and tufts of setae. Carpus with row of small tubercles each with short setae on dorsolateral margin, lateral surface with sparse low tubercles and tufts of setae;

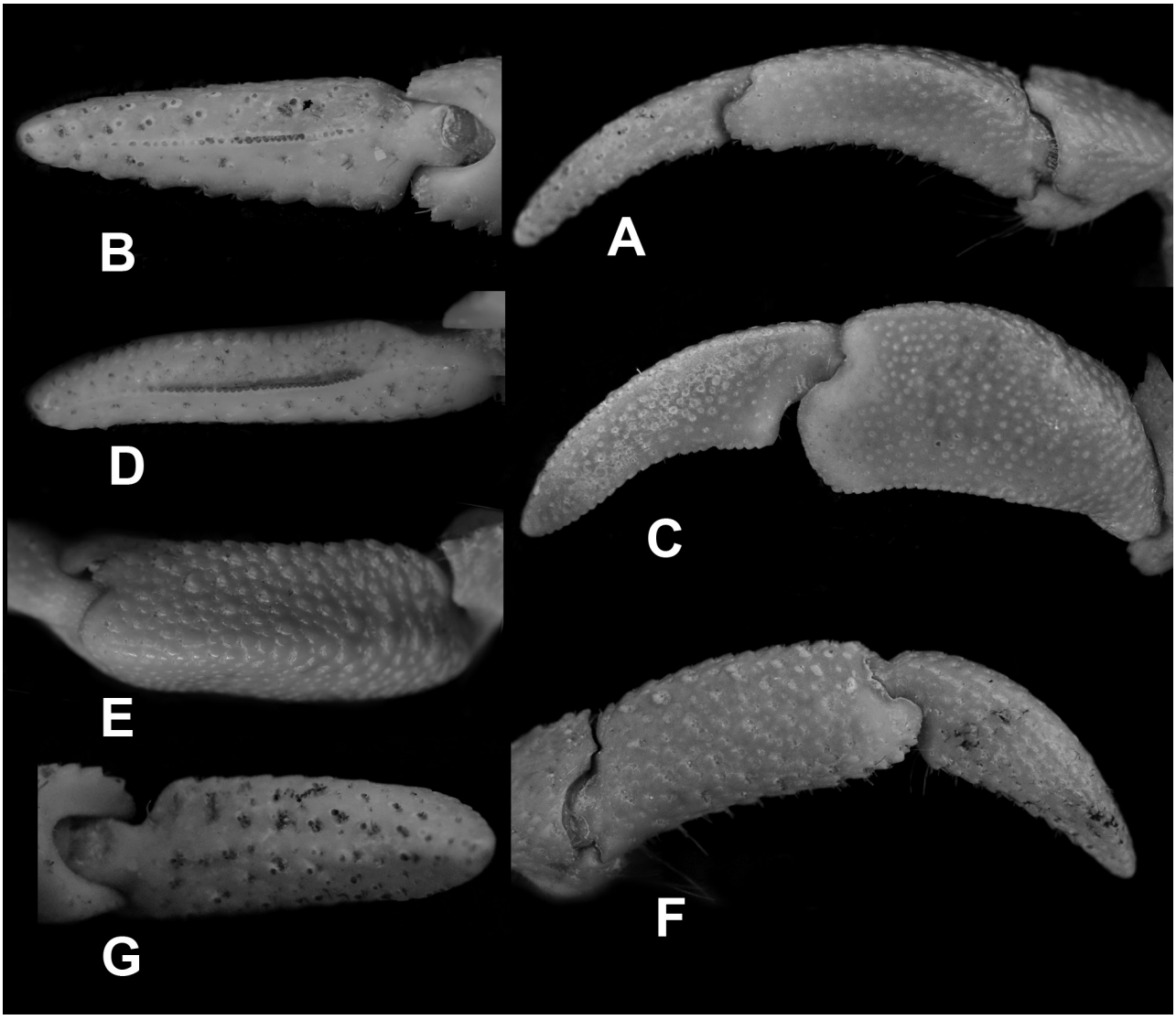

Fig. 16. *Coenobita granularis* n. sp. Holotype ♂ (SL 10.4 mm, MZB Cru 5729). A, dactylus and propodus of left P2, lateral view; B, dactylus of left P2, ventral view; C, dactylus and propodus of left P3, lateral view; D, dactylus of left P3, ventral view; E, propodus of left P3, dorsal view; F dactylus and propodus of right P3, lateral view; G, dactylus of right P3, ventral view.

mesial surface compressed, smooth except for some tufts of setae. Merus compressed laterally and mesially, transverse row of flattened tubercles on lateral surface; mesial surface almost smooth, tufts of long setae on dorsal and ventral margin. Right P3 slightly more slender than left. Dactylus and propodus (Fig. 16F) covered by with flattened tubercles; mesial and ventral surfaces of dactylus (Fig. 16G) with low corneous-tip tubercles; mesial surface of propodus with transverse rows of corneous-tip small tubercles. Carpus and merus as in left P3.

P4 semi-chelate (Fig. 15C), dactylus with row of small corneous teeth ventrally, long, coarse setae dorsally; propodal rasp well developed, occupying large, circular area, consisting of numerous corneous scales; propodus with distodorsal spine. P5 chelate.

In male, coxae of P5 thick, each forming calcified sexual tube, right tube long, directed to left, left tube short, broader than right. Gonopore positioned on moderately broad with truncate tip posterior projection or papillae, with short, sparse, setae; cylindrical, small, sternal protuberance between both coxae (Figs. 14D, F, 15D, E). In females, coxae of P5 thick, subquadrate.

Telson (Fig. 15E) with distinct lateral indentation, separating anterior and posterior lobes. Anterior lobe as long as posterior. Posterior lobes slightly asymmetrical separated by narrow median cleft; margins rounded, with row of setae.

Variation: Morphological variation related to sex is observed in the degree of tuberculation and the density of setae on the chelipeds and ambulatory legs. In one female specimen (MZB Cru 5730), the tubercles on the ambulatory legs are larger and more pronounced, and the setae are denser. The left sexual tube of the holotype forms a sharp corner laterally near the truncated tip (Fig. 14D), while in the paratypes, the lateral margin is oblique near the truncated tip (Fig. 14F). It is possible that the holotype sexual tube is damaged or worn out, as it is also devoid of setae.

Color in life: General light brown, orangish brown or dark brown (Fig. 17). Shield light brown or orangish brown with streak of green, darker brown dorsodistally. Ocular peduncles green or dark brown, corneas black. Antennal peduncles dark brown, with fifth segment dark orange. Antennular peduncles dark brown, with penultimate segment dark orange. Chelipeds with palms and dactyli light brown or orangish brown, cutting edges white; carpi and meri light brown or orangish brown. P2 and P3 with dactyli and propodi light brown; carpi and meri greenish brown or light brown tinge with dark brown.

Size: Largest male SL 11.5 mm; largest female 10.9 mm.

Etymology: The name is derived from the Latin word "*granular*," meaning "small grain", referring to the tuberculate surface of the chelipeds and pereopods in most specimens, especially in adults.

Ecological notes: In Central Sulawesi, the habitat consists of sandy beaches with low shrubs, and the beach typically features a shallow intertidal zone. This species is sympatric with *C. pseudorugosus* (Table 1; Shih et al. 2023a) and *C. rugosus*, but individuals of *C. granularis* usually congregate separately from the other two species.

Distribution: Indonesia (Gulf of Tomini, Central Sulawesi).

Remarks: Among the species with row of a stridulatory ridge on the left cheliped palm in *Coenobita*, this new species most closely resembles *C. perlatus*, *C. pseudorugosus*, and *C. purpureus* Stimpson, 1858 in having distinctly unequal sexual tube with the right tube being more slender and much longer than the left. The morphological similarity between *C. granularis* n. sp. and *C. pseudorugosus* is also supported by molecular evidence (Fig. 23).

In *C. granularis* and *C. perlatus*, the right sexual tube is 2 times as long as the left. However, the shape of the left sexual tube differs between the two species. In the new species, the left sexual tube is broad and stout, about 1.3 times as long as broad (measured along the mesial margin), and the sternal protuberance is small and ovate (Figs. 14D, F, 15D, E), while it is more slender, about 1.5 times as long as broad, sternal protuberance rounded, small in *C. perlatus* (Alcock 1905: pl. 14(2a); Nakasone, 1988: fig. 5F). In *C. pseudorugosus* and *C. purpureus*, the right sexual tube is shorter, about 1.6 and 1.2 times as long as the left respectively. The left sexual tube of *C. pseudorugosus* is 1.1 times as long as broad, the sternal protuberance is ovate and relatively small (Nakasone 1988: fig. 1H; Shih et al. 2023a: figs. 6B, 9A, C, E). In *C. purpureus* the left tube is 1.8 times as long as broad and the sternal protuberance is ovate and relatively large (Nakasone 1988: fig. 4F).

Other differences observed include the left cheliped of *C. granularis*, which has a covering of flattened tubercles on the outer surface of the palm (Figs. 15A, 17D–F) [covered by large tubercles in *C. perlatus* (Nakasone 1988: fig. 5B) and *C. pseudorugosus* (Nakasone 1988: fig. 1C; Shih et al. 2023a: figs. 6E, 8A, C, E, G); with sparser tubercles on the outer upper surface and almost smooth on the lower outer surface in *C. purpureus* (Nakasone 1988: fig. 4B)]. The left P3 propodus is broad, with the dorsal margin not delimited by a row of tubercles; the lateral surface is slightly convex and punctate in *C. granularis* (Fig. 16C, E) [in *C. perlatus*, the dorsolateral margin of the P3 propodus is not delimited, and the lateral surface is convex and

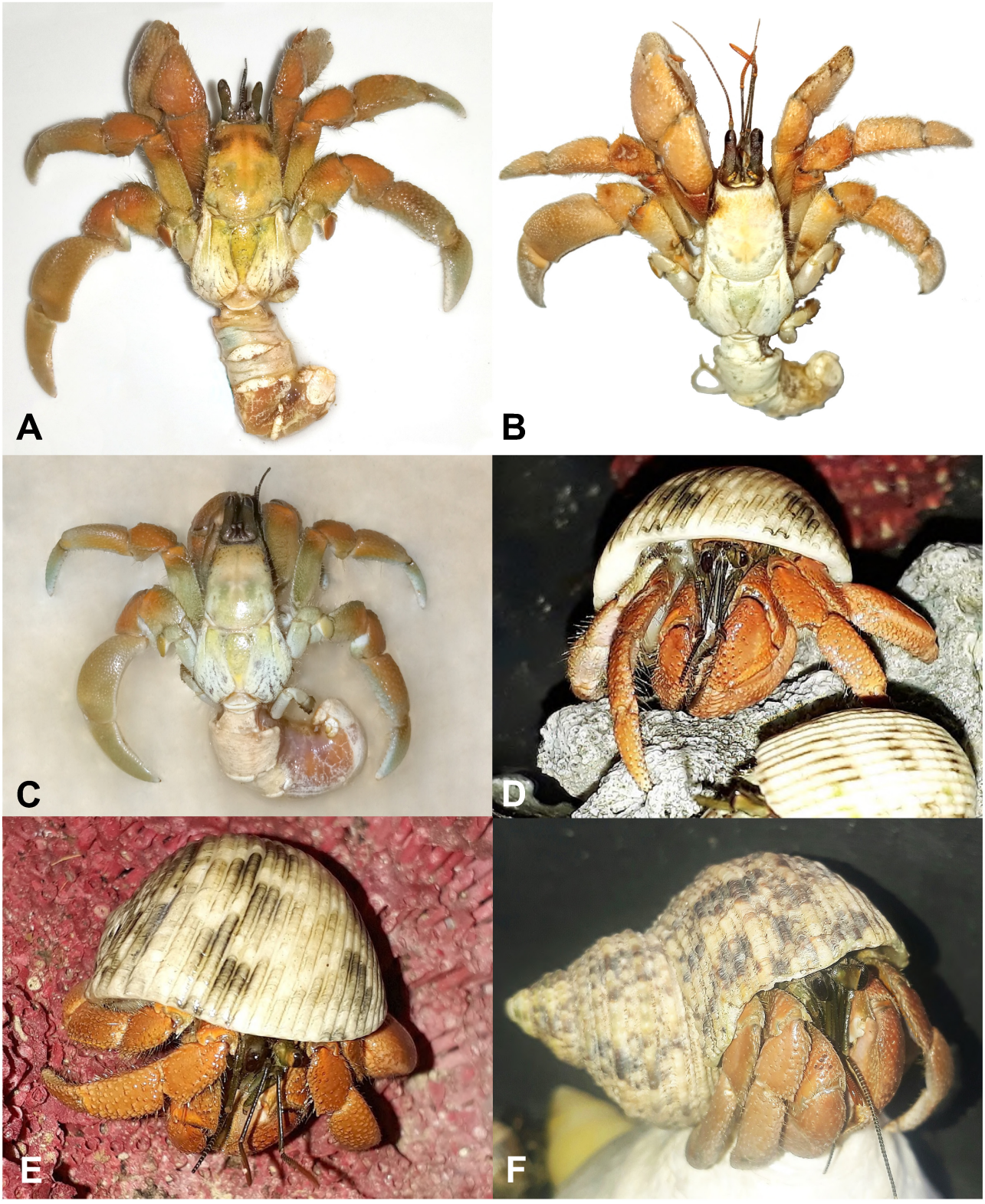

Fig. 17. Color in life of *Coenobita granularis* n. sp. C, tissue sample (see Table 1), TS COx95. A, B, D–F, specimens not kept. All specimens from Central Sulawesi, Indonesia.

covered with low tubercles (Nakasone 1988: fig. 5C); in *C. pseudorugosus*, the dorsolateral margin of the P3 propodus is delimited by a longitudinal ridge of small tubercles, with the lateral surface smooth and the dorsal margin broader distally (Nakasone 1988: fig. 1E; Shih et al. 2023a: figs. 6G, 7, 10A, C, E, 11A, C, E, G, I, K); in *C. purpureus*, the dorsolateral margin of the P3 propodus is delimited by a strong ridge consisting of tubercles, with the lateral surface slightly convex and punctate (Nakasone 1988: fig. 4C)]. Furthermore, the coloration of these four species is different: *C. granularis* is light brown or orangish brown (Fig. 17), *C. pseudorugosus* is light and dark brown (Shih et al. 2023a: fig. 7), *C. perlatus* is dark red or bright red (Schäfer 2020: image on p. 93), while *C. purpureus* is purple (Shih 2020: figs. 209, 210).

Coenobita variabilis McCulloch, 1909

(Figs. 18–21)

Cenobita rugosa – Heller 1865: 82 (Sydney, Australia). (not *Coenobita rugosus* H. Milne Edwards, 1837).

Cenobita olivieri – Haswell 1882: 160–161 (N. W. Coast of Australia). (not *Coenobita olivieri* Owen, 1839).

Coenobita spinosus variabilis McCulloch, 1909: 305–306, pl. 88 (2, 2a) (type locality: Cape York, N Queensland, Australia); Springthorpe and Lowry 1994: 91 (syntypes).

Coenobita spinosus – Morgan 1987: 167 (North Territory, N Australia); Morgan 1990: 8 (NW Australia). (not *Coenobita spinosus* H. Milne Edwards, 1837).

Coenobita variabilis – Harvey 1992: 196–209, figs. 2–6 (Darwin, Northern Territory, Australia); Jones and Morgan 1994: 123, 4 unnumbered figs. (N Australia); Davie 2002: 35; Davie 2005: 149 (Bentinck Is., N Queensland, Australia); McLaughlin et al. 2010: 16; Tan et al. 2018: 322, 324 (mitogenome); Wang et al. 2019: 2646 (mitogenome); Gong et al. 2020: 1805, 1810 (mitogenome); Schäfer 2020: 106–107, 2 unnumbered figs.; Sasaki 2023: 6404 (list).

Material examined: **West Papua, Indonesia**: 4 ♂♂ (16.8, 17.0, 18.2, 18.2 mm) (NCHUZOOL 15257), 2 ♂♂ (19.7, 21.8 mm) (NCHUZOOL 15258), 2022.

Additional material: **Australia**: 4 ♂♂ (5.8, 7.7, 11.1, 11.8 mm), 2 ♀♀ (5.5, 8.6 mm) (QM W21232), West Governor Is., NW side, Napier Broome Bay, Kimberley Coast, WA, coll. J. Short, 26 Nov. 1995; 7 ♂♂ (10.2, 10.4, 10.8, 11.6, 11.8, 11.9, 16.4 mm) (QM W20272), Bedford Is., Kimberley coast, WA, coll. J. Short, 19 Nov. 1994; 1 ♂ (12.8 mm) (QM W9028), 1 ♀ (7.9 mm) (QM W9025), mouth of E. Alligator R., NT, coll. P. Davie, 30 Apr. 1979; 1 ♀ (13.7 mm) (QM W9091), West Alligator R., NT, 30 Apr. 1979; 2 ♂♂ (9.8, 14.7 mm) (QM W23491), Karumba Pt, Cape York Peninsula, Far North QLD, coll. T. Stevens, 24 Nov. 1993.

Diagnosis: Shield (Figs. 18A, 21A), transversely convex, about 1.7 times as long as broad; dorsal surface punctate. Ocular peduncles reaching third proximal of ultimate article of antennular peduncles; basal article of antennular peduncles 0.8 times as long as penultimate article (Fig. 18B); antennal peduncles (Fig. 18C) exceeding ocular peduncles by half length of fifth article, second article stout, short, with flattened tubercles. Chelipeds (Fig. 19A, C) unequal and dissimilar, left larger than right, brush of setae on half proximal of upper margin of both palms; left cheliped palm with row of 5–6 small and large stridulatory apparatus (laminar ridge) on upper outer surface, outer surface with widely-spaced tubercles, sometimes corneous-tipped; lower margin of palm sinuous; lower proximal angled rounded. Merus of both chelipeds each with a dense tuft of bristles on middle lower inner margin (Fig. 19B, D), comparatively sparse in left one. Left P2 and P3 dissimilar (Fig. 20A, C), P2 more slender than P3. Lateral surfaces of dactylus and propodus of left P2 (Fig. 20A) punctate or with sparse flattened tubercles, ventral surface of dactylus (Fig. 20B) with longitudinal ridge consisting of row of closely-spaced tiny corneous teeth proximally, widely-spaced distally. Right P2 slightly shorter, armament similar. Left P3 (Fig. 20C–E) with lateral surfaces of dactylus and propodus broad, smooth, sparsely punctate; ventral surface of dactylus slightly concave, median longitudinal ridge consisting of row of tiny corneous teeth, closely-spaced proximally, widely-spaced distally. Right P3 (Fig. 20F) slightly more slender than left. Dactylus and propodus (Fig. 20F) densely punctate; ventral surface of dactylus (Fig. 20G) with low corneous-tip tubercles. In male, coxae of P5 thick, each forming calcified sexual tube, left tube narrower than right; small, subtriangular sternal protuberance between both coxae (Figs. 18D, 19F). Telson (Fig. 18E) posterior lobes slightly asymmetrical, separated by narrow median cleft; margins truncate, with row of setae.

Variation: The stridulatory apparatus row on the outer surface of the palm of the left cheliped is variable (Fig. 19A), being either distinct or indistinct, and this variation is not related to the sex or size of the individual. The sexual tubes are nearly the same length (Figs. 18D, 19F), although in some individuals, the tubes are slightly unequal.

Color in life (Fig. 21): Whole body and pereopods typically brown, with variations including light brown and reddish-brown. Palms of chelipeds with outer surface darker than other parts of body.

Size: Largest male SL 21.8 mm; largest female: 13.7 mm.

Ecological notes: According to the local people in West Papua, the habitat consists of sandy beaches, often near river estuaries and bordered by jungle with

a humus substrate. Compared to *C. brevimanus*, larger individuals of this species tend to inhabit the humus area closer to the coastline, while smaller ones are typically found nesting under piles of rocks or dead corals on the sandy beach. This species tends to live further inland compared to *C. perlatus*.

Distributions: Northern part of Australia to the western (Indonesian) part of New Guinea Island, particularly along the coastline of the Arafura Sea in South Papua Province.

Remarks: *Coenobita variabilis* is similar to *C. scaevola* in having a tuft of bristles on the middle of the lower inner margin of the right cheliped merus (Figs. 19D, 22D). However, *C. variabilis* differs in the following characters: 1) with a variable stridulatory apparatus row on the outer surface of the left cheliped palm (Fig. 19A) [vs. a regular row of stridulatory apparatus in *C. scaevola* (Fig. 22A)]; 2) sexual tubes nearly the same length or slightly unequal (Figs. 18D, 19F) [vs. right sexual tube robust, longer than left, curved laterally in *C. scaevola* (Fig. 22C)]; and 3) a bristle tuft on the middle of the lower inner margin of the left cheliped merus in large specimens (Fig. 19B) [vs. none in *C. scaevola* (Fig. 22B)].

Regarding the bristle tuft on the left cheliped merus of *C. variabilis*, all specimens from West Papua exhibit this distinct character, whereas it only appears in some from Australia (*e.g.*, QM W23491, QM W21232, QM W23491). This character is presumed to typically appear in large males (all specimens from West Papua are large males with SL 16.8–21.8 mm), but it is inconsistent in smaller individuals (all Australian specimens with SL ≤ 16.4 mm). In other Australian literature, the sizes reported were also smaller (*e.g.*, SL 14.3 mm in Morgan 1987; SL 11.1 mm in Morgan 1990). Notably, Jones and Morgan (1994) mentioned

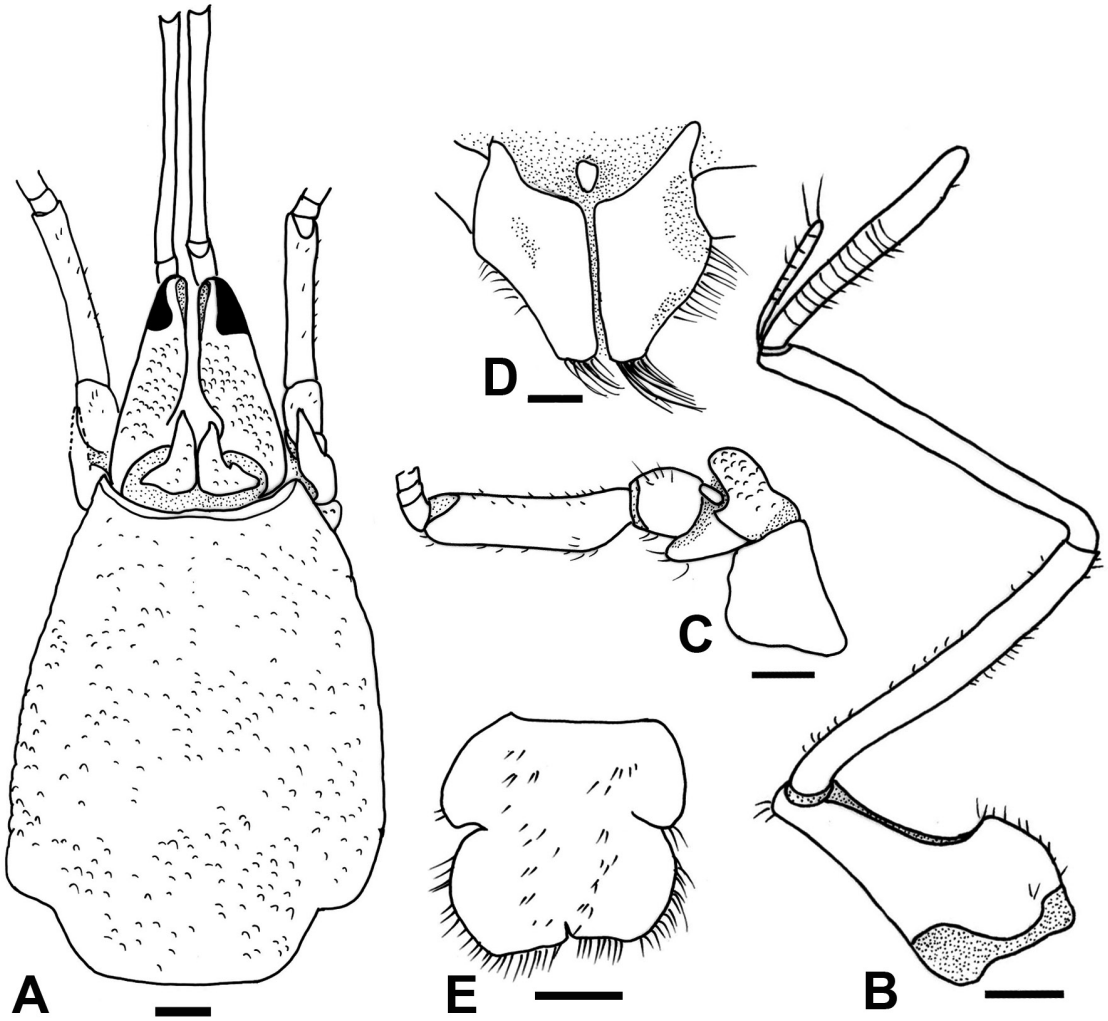

Fig. 18. *Coenobita variabilis* McCulloch, 1909, ♂ (SL 16.8 mm, NCHUZOOL 15257). A, shield and cephalic appendages; B, right antennular peduncles, lateral view; C, right antennal peduncles, lateral view; D, F, sternite and coxae of male P5; E, telson. Setae partially omitted. Scale bars: A–E = 2 mm.

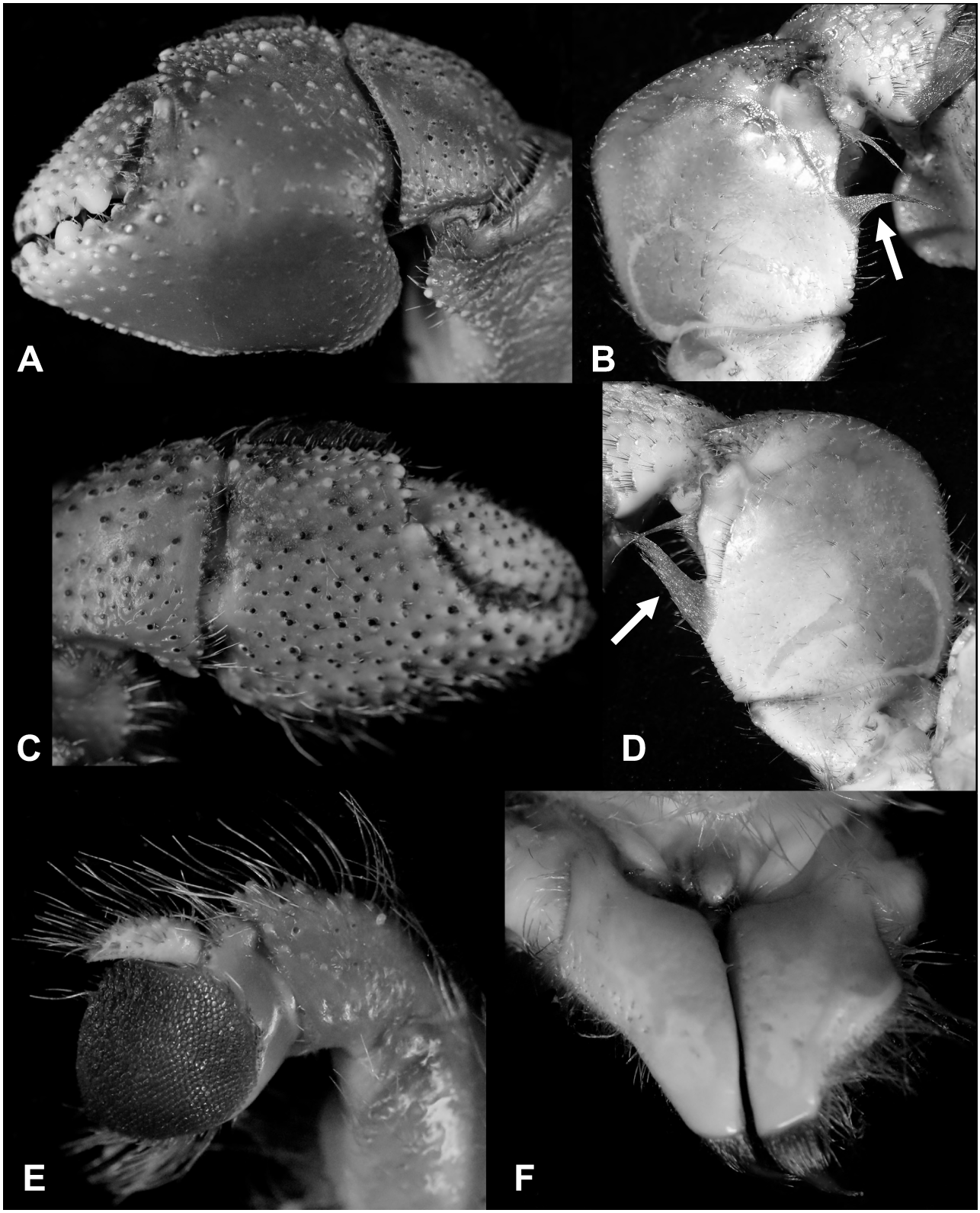

Fig. 19. *Coenobita variabilis* McCulloch, 1909, ♂ (SL 16.8 mm, NCHUZOOL 15257). A, left cheliped, outer view; B, merus of left cheliped, inner view, showing the setal tuft (arrowed); C, right cheliped, outer view; D, merus of right cheliped, inner view, showing the setal tuft (arrowed); E, left P4, lateral view; F, sternite and coxae of male P5.

a carapace length of about 40 mm. This may suggest that suitable habitats for Australian populations are comparatively limited.

Coenobita variabilis was generally thought to be endemic to Australia (*e.g.*, Davie 2005; Schäfer 2020). However, McCulloch (1909) included other localities near Papua New Guinea (Muray Islands and Torres Straits), as well as Vanuatu (New Hebrides) and Fiji. It is, therefore, not unexpected that the distribution of this species has extended to the southern coast of West Papua, Indonesia.

Molecular analyses

A 545 bp segment of the 16S rDNA and a 658 bp segment of *COI* from specimens (or tissue samples), including 16 from *C. moluccensis*, 36 from *C. patsyae* (16S failed for NCHUZOOL 15274), 9 from *C. celebensis*, 20 from *C. granularis*, and 7 from *C. variabilis*, were amplified and aligned (Table 1). A total of 34 haplotypes of the 16S and 71 haplotypes of *COI* were found for the above species (Table 1). The phylogenetic tree (Fig. 23), based on the combined 16S and *COI* data, was constructed using ML analysis, with respective support values from the BI analysis. Support values greater than 50% are shown. The tree shows that the four new species and *C. variabilis* are well-supported by both ML and BI methods. While *C. patsyae*, *C. moluccensis*, and *C. celebensis* are closely related and sister to *C. lila*, *C. granularis* is a sister species to *C. pseudorugosus*. The Indonesian and Australian sequences of *C. variabilis* form a well-supported clade.

A total of 61 specimens of *C. moluccensis*, *C.*

Fig. 20. *Coenobita variabilis* McCulloch, 1909, ♂ (SL 16.8 mm, NCHUZOOL 15257). A, dactylus and propodus of left P2, lateral view; B, dactylus of left P2, ventral view; C, dactylus and propodus of left P3, lateral view; D, dactylus of left P3, ventral view; E, propodus of left P3, dorsal view; F dactylus and propodus of right P3, lateral view; G, dactylus of right P3, ventral view.

patsyae, *C. celebensis* were used to construct the 16S+*COI* haplotype network (Fig. 24). There are 11 haplotypes in *C. moluccensis*, 28 in *C. patsyae*, and 8 in *C. celebensis*. Three clade can be clearly separated by 16S+*COI*: *C. celebensis* differs from *C. patsyae* by ≥ 25 bp and from *C. moluccensis* by ≥ 32 bp, with ≥ 39 bp differences between *C. patsyae* and *C. moluccensis*. The pairwise nucleotide divergences and total bp number differences of *COI* within and between the related species are shown in table 3. The genetic

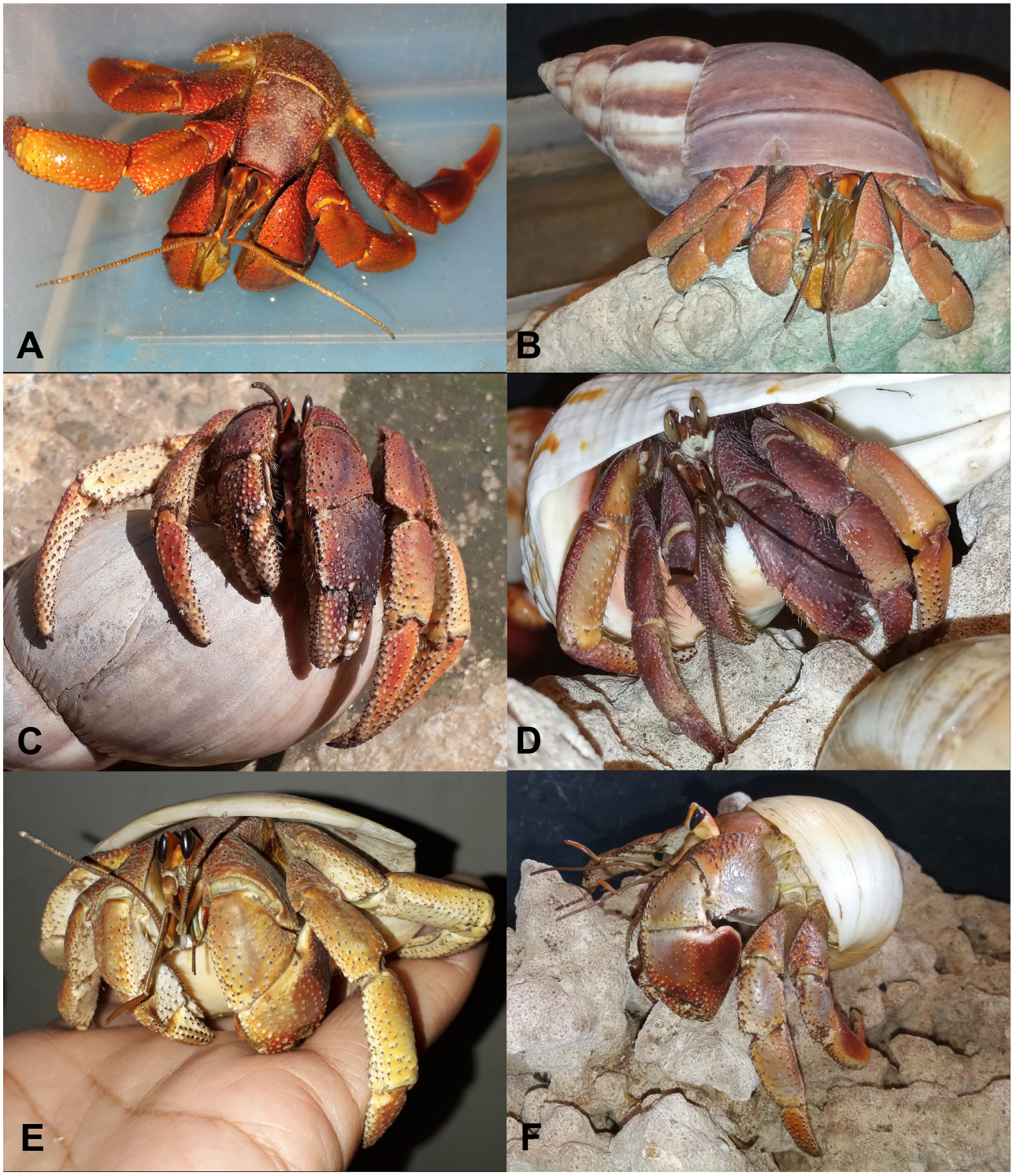

Fig. 21. Color in life of *Coenobita variabilis* McCulloch, 1909. All specimens from West Papua, Indonesia; not kept.

distances (and bp differences) are 0–3.3% (0–21 bp) within species, and 3.6–17.39% (23–100 bp) between species.

DISCUSSION

Integrative taxonomy and genetic divergence

Species in the genus *Coenobita* have long been traded as ornamental crustaceans. They are attractive to hobbyists due to their beautiful coloration and the ease of keeping them alive in a terrarium (Bundhitwongrut 2018; Schäfer 2020). However, detailed taxonomic studies of this genus are limited. In the last 50 years, only two new species have been described, *Coenobita pseudorugosus* Nakasone, 1988 and *C. lila* Rahayu, Shih & Ng, 2016, with molecular support available for the latter. The identities of *C. pseudorugosus* and *C. longitarsis* have recently been confirmed by both morphological and molecular evidence (Shih et al. 2023a).

Integrative taxonomy has become crucial in delineating species because it utilized multiple

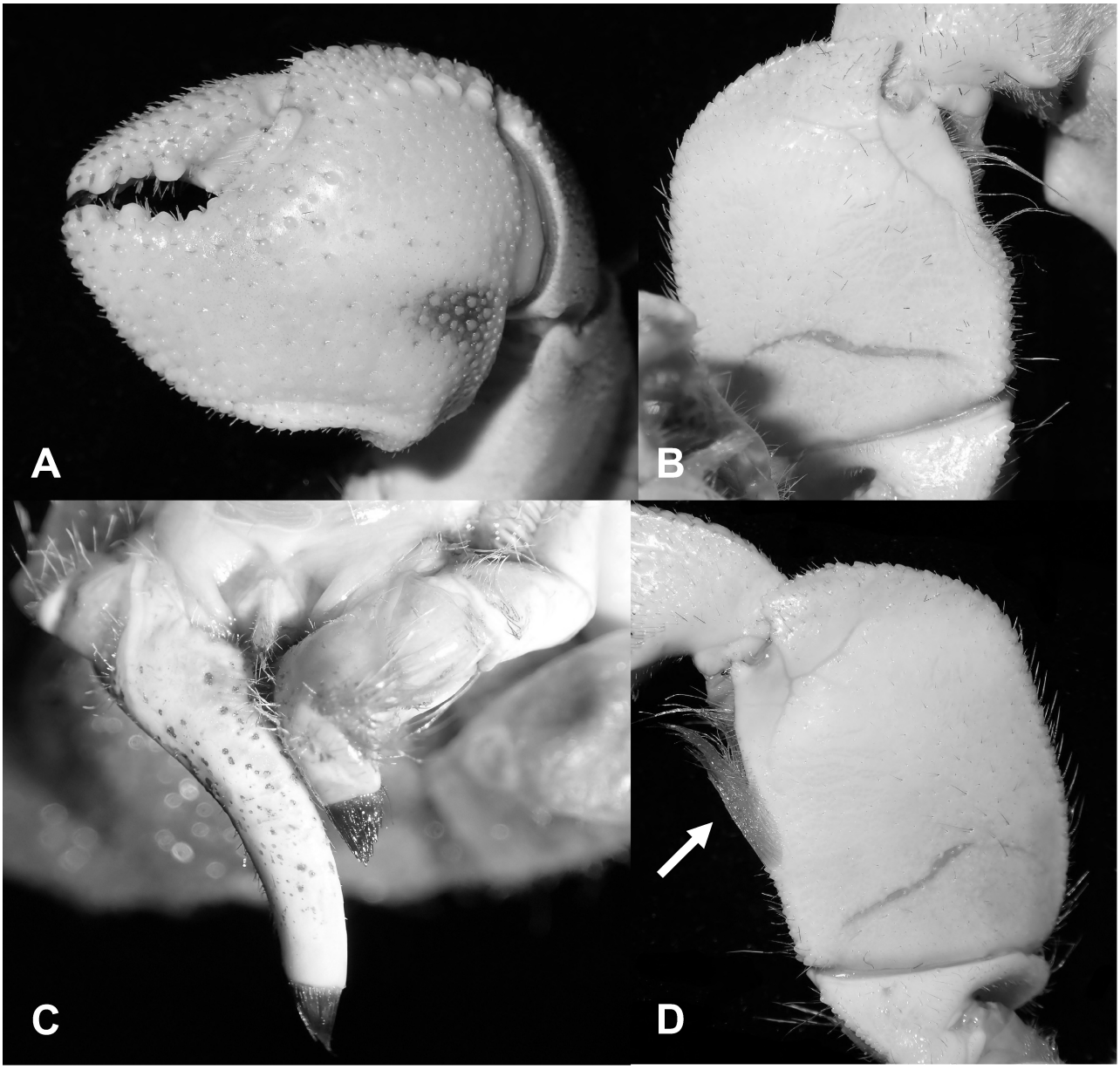

Fig. 22. *Coenobita scaevola* (Forskål, 1775), ♂ (SL 16.8 mm, ZRC 2017.0642). A, dactylus and propodus of left P2; B, merus of left cheliped, inner view; C, sternite and coxae of male P5; D, merus of right cheliped, inner view, showing the setal tuft (arrowed).

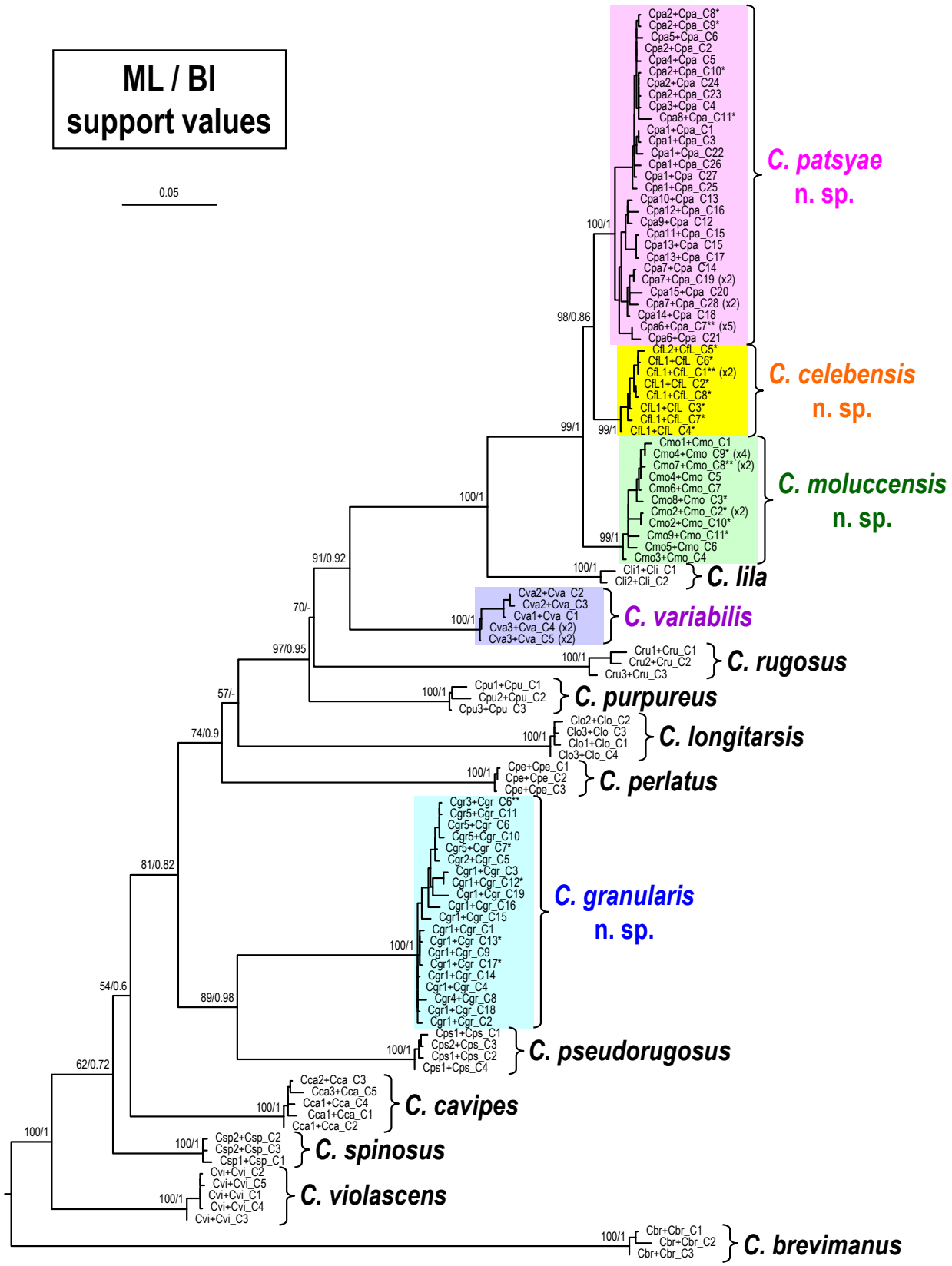

Fig. 23. A maximum likelihood (ML) tree for *Coenobita* species from the Indo-West Pacific, based on the combined 16S rDNA and cytochrome *c* oxidase I genes. Probability values at the nodes represent support values for ML and Bayesian inference (BI). For haplotype names, see table 1.

characters, including DNA and various other data types, to delimit, discover, and identify meaningful, natural species and taxa at all levels (Dayrat 2005; Will et al. 2005; Padial et al. 2010; Goldstein and DeSalle 2011; Pante et al. 2015). Recent examples of integrative taxonomy in decapod crustaceans (*e.g.*, Yuan et al. 2022; Shih et al. 2023c 2024). In our study, while the morphological differences among *C. moluccensis*, *C. patsyae*, and *C. celebensis* are considered minor (Table 2), molecular evidence plays an crucial role in distinguishing them, particularly regarding genetic distances (Table 3) and monophyly (Figs. 23, 24).

The interspecific divergences of the DNA barcode gene *COI* among the species examined in this study are ≥ 3.6% (K2P distance) (Table 3). Within the species complex composed of *Coenobita moluccensis*, *C. patsyae*, and *C. celebensis*, the minimum interspecific divergences are smaller compared to values > 10% found in other coenobitid studies (*e.g.*, 13.37% in Rahayu et al. 2016; 13.5% in Hamasaki et al. 2017; 10.18% in Shih et al. 2023a). However, these values are closer to the 4% range observed in the coastal hermit crabs *Calcinus* (Malay and Paulay 2010). Additionally, the three species are strongly supported in the phylogenetic tree (Fig. 23) and haplotype network (Fig. 24). As a result, they can be considered as pseudocryptic species (see Ng and Shih 2023; Shih et al. 2023a b c; Thurman et al. 2023) due to their similar morphology.

Phylogeny and morphological and color traits

Based on the phylogeny constructed from the

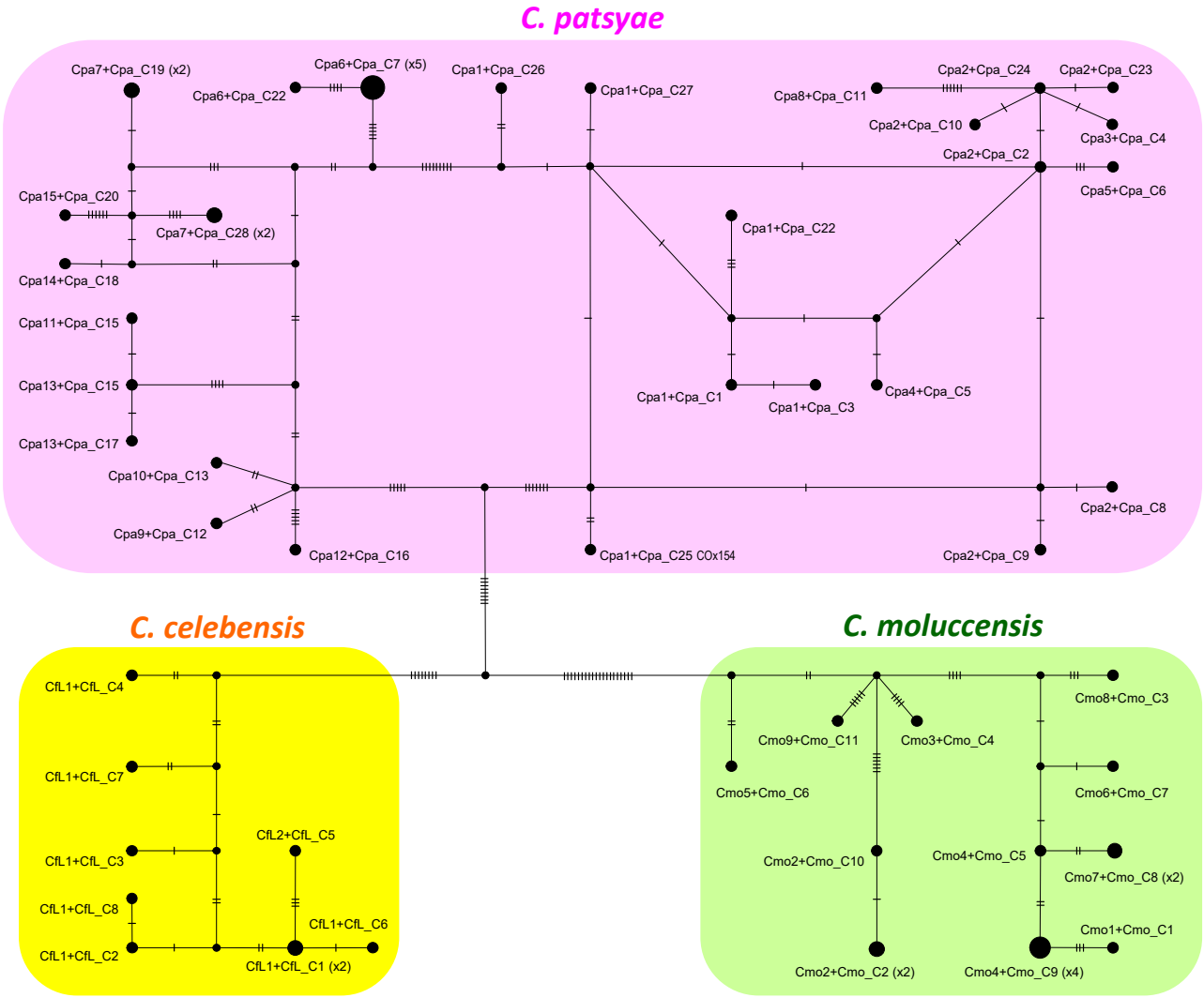

Fig. 24. Haplotype network for the 16S+*COI* haplotypes observed from *Coenobita patsyae* n. sp., *C. celebensis* n. sp., and *C. moluccensis* n. sp. Unlabeled nodes represent inferred haplotypes not found in the sampled populations, and the hatch marks indicate the number of mutations. See table 1 for haplotype names.

available sequences of the combined 16S and *COI* (Fig. 23), *C. moluccensis*, *C. patsyae*, and *C. celebensis* form a highly supported major clade that is sister to *C. lila*. Their close genetic relationship is also reflected in their similar morphology and coloration (Table 2), including the absence of a stridulatory ridge on the outer surface of the left chela (Figs. 2A, 4, 6A, 8, 10A, 12; Rahayu et al. 2016: figs. 2A, 4A–C, 10), the short sexual tubes in males (Figs. 1D, 2D, 5D, 6D, 9D, 10D; Rahayu et al. 2016: figs. 1D, 2G), and the yellow or orange tinges on the pereopods (see Remarks under *C. celebensis*). *Coenobita patsyae* and *C. celebensis* from Sulawesi are more closely related to each other, forming a clade with slightly weaker support that is sister to *C. moluccensis* from Aru Island, Maluku. Similarly, *C. granularis* shares morphological similarities with *C. pseudorugosus*, as supported by the molecular phylogeny that places them as sister species. However, although *C. perlatus* and *C. purpureus* exhibit morphological similarities to these two species, their relationships are more distant (Fig. 23), suggesting that these shared traits may have evolved convergently.

Coenobita moluccensis, *C. patsyae*, and *C. celebensis* exhibit varying degree of yellow or orange coloration on the cheliped meri, and even on the second and third pereopods (Figs. 4, 8, 12). In *C. lila*, a very faint yellow tinge is also present on the pereopods (Rahayu et al. 2016: figs. 10, 11A–C). According to the phylogenetic tree (Fig. 23), the presence of yellow or orange coloration on the cheliped meri and other pereopods is likely a derived trait in these closely related species. Some individuals of *C. patsyae* have brightly yellow or orange cheliped meri (Fig. 8D), which are very similar to those in *C. celebensis* (Fig. 12), suggesting a closely relationship between them, as supported by the phylogenetic tree and haplotype network (Figs. 23, 24).

Species discovery and geographic distribution

In our study, four new species and one newly recorded species of *Coenobita* are reported from Indonesia, increasing the total number of recognized species in this country to 13: *C. brevimanus*, *C. cavipes*, *C. celebensis*, *C. granularis*, *C. lila*, *C. longitarsis*, *C. moluccensis*, *C. patsyae*, *C. perlatus*, *C. pseudorugosus*, *C. rugosus*, *C. variabilis*, and *C. violascens*. Consequently, Indonesia stands out as the global hotspot with the highest species diversity for this genus, a pattern similar to that observed in other marine organisms (Veron et al. 2009; Siallagan et al. 2023). Notably, six of these species, viz. *C. celebensis*, *C. granularis*, *C. patsyae*, *C. pseudorugosus*, *C. rugosus*, and *C. violascens*, can be found within the Gulf of Tomini, Central Sulawesi (Shih et al. 2023a; this study), suggesting that unique habitat conditions in this area may contribute to speciation within the genus. It is recommended that further studies on larval ecology (*e.g.*, Hamasaki et al. 2015 2018; Doi et al. 2018), population ecology (*e.g.*, Barnes 2002 2003; Bundhitwongrut et al.

Table 3. Matrix of the percentage of pairwise nucleotide divergences with Kimura 2-parameter (K2P) distances and the number of basepair (bp) differences based on the cytochrome *c* oxidase subunit I (*COI*) gene within and between the new species (and new record) of *Coenobita* in this study and their closely related species. In the interspecific (right) part of the table, lower-left values represent K2P distances and upper-right values indicate bp differences. Range of values are given in parentheses

	Intraspecific		Interspecific						
	Nucleotide divergence	Mean nucleotide difference	*C. patsyae*	*C. celebensis*	*C. moluccensis*	*C. lila*	*C. variabilis*	*C. granularis*	*C. pseudorugosus*
C. patsyae	1.22 (0–3.3)	7.86 (0–21)		30.38 (23–35)	33.03 (23–39)	66.74 (61–70)	65.66 (60–69)	91.66 (84–97)	93.38 (87–97)
C. celebensis	0.86 (0.15–1.39)	5.6 (1–9)	4.81 (3.6–5.58)		31.23 (23–35)	65 (63–67)	71.88 (67–75)	94.66 (89–100)	94.42 (91–98)
C. moluccensis	1.14 (0–2.02)	7.36 (0–13)	5.27 (3.61–6.29)	4.96 (3.61–5.6)		65.25 (60–69)	60.92 (57–65)	94.76 (88–100)	92.91 (88–96)
C. lila	1.08	7	11.21 (10.14–11.83)	10.87 (10.5–11.23)	10.96 (9.99–11.67)		78.57 (78–79)	91.7 (87–95)	85.5 (83–88)
C. variabilis	0.98 (0–1.86)	6.38 (0–12)	10.99 (9.94–11.62)	12.12 (11.2–12.72)	10.12 (9.4–10.87)	13.41 (13.3–13.49)		84.85 (78–90)	85.5 (84–87)
C. granularis	1.35 (0–2.33)	8.77 (0–15)	15.67 (14.17–16.74)	16.25 (15.13–17.33)	16.33 (14.98–17.39)	15.7 (14.77–16.37)	14.37 (13.05–15.37)		76.64 (72–83)
C. pseudorugosus	0.64 (0.46–0.92)	4.17 (3–6)	16.03 (14.77–16.74)	16.22 (15.54–16.93)	15.97 (14.99–16.61)	14.43 (13.96–14.92)	14.47 (14.17–14.77)	12.9 (12.02–14.13)	

2014), and population genetics (*e.g.*, Hamasaki et al. 2017), as these areas of research may help to elucidate the mechanisms of sympatry and provide valuable insights for conservation efforts. Considering that *Coenobita* species from other regions of Indonesia have not been well studied, we anticipate that more species may be discovered in the future.

CONCLUSIONS

In our study, we confirmed the existence of four new species, viz. *C. moluccensis* n. sp., *C. patsyae* n. sp., *C. celebensis* n. sp., and *C. granularis* n. sp., as well as one newly recorded species, *C. variabilis*, in Indonesia. This confirmation is based on the integration of morphological characters and molecular evidence derived from mitochondrial 16S and *COI* markers. Notably, *C. moluccensis*, *C. patsyae*, and *C. celebensis*, supported by genetic evidence, form a major clade that can be considered as a species complex. This complex is closely related to *C. lila*, with which it shares morphological similarities. Additionally, *C. granularis* and *C. pseudorugosus* exhibit similar morphological traits and are identified as sister species in our analysis. The discovery of *C. variabilis* in West Papua, Indonesia, expands its known distribution from Australia to New Guinea Island. Our research increases the total number of *Coenobita* species documented in Indonesia to 13. This highlights the effectiveness of integrative taxonomy in confirming the existence of distinct species and contributes to our understanding of the biodiversity of *Coenobita* in Indonesia. Moreover, it underscores the importance of considering multiple sources of data in species identification and classification.

Acknowledgments: This study was supported by a grant from the National Science and Technology Council (NSTC 112-2313-B-005-051-MY3), Executive Yuan, Taiwan, to HTS. We thank Min-Wan Chen for helping part of the molecular work; Peter Davie and Marissa McNamara for loaning specimens in QM; and Choi Sin Tung (Tony Choi) for providing useful information. We also acknowledge the two anonymous referees who helped improve the manuscript.

Authors' contributions: HTS conceived this study, morphological description, molecular analysis, and drafted the manuscript. DLR performed the morphological description, line drawings, and drafted the manuscript. FAP provided the specimens, performed the ecological observation and color in life, and drafted the manuscript. All authors read and approved the final manuscript.

Competing interests: The authors declare that they have no conflict of interest.

Availability of data and materials: Sequences generated in the study were deposited into the GenBank database (accession numbers in Table 1).

Consent for publication: Not applicable.

Ethics approval consent to participate: Not applicable.

REFERENCES

Alcock A. 1905. Catalogue of the Indian Decapod Crustacea in the Collection of the Indian Museum. Part II. Anomura. Fasciculus I. Pagurides. Trustees of the Indian Museum, Calcutta, India, xi+193 pp., 16 pls.

Barnes DKA. 2002. Ecology of subtropical hermit crabs in SW Madagascar: refuge-use and dynamic niche overlap. Mar Ecol Prog Ser **238:**163–172. doi:10.3354/meps238163.

Barnes DKA. 2003. Ecology of subtropical hermit crabs in SW Madagascar: short-range migrations. Mar Biol **142:**549–557. doi:10.1007/s00227-002-0968-5.

Bellwood DR, Meyer CP. 2009. Searching for heat in a marine biodiversity hotspot. J Biogeogr **36:**569–576. doi:10.1111/j.1365-2699.2008.02029.x.

Bundhitwongrut T. 2018. Unregulated trade in land hermit crabs in Thailand. Nat Hist Bull Siam Soc **63:**27–40.

Bundhitwongrut T, Thirakhupt K, Pradatsundarasar Ao. 2014. Population ecology of the land hermit crab *Coenobita rugosus* (Anomura, Coenobitidae) at Cape Panwa, Phuket Island, Andaman coast of Thailand. Nat Hist Bull Siam Soc **60:**31–51.

Crandall KA, Fitzpatrick Jr JFJ. 1996. Crayfish molecular systematics: Using a combination of procedures to estimate phylogeny. Syst Biol **45:**1–26. doi:10.1093/sysbio/45.1.1.

Davie PJF. 2002. Crustacea: Malacostraca: Eucarida (Part 2): Decapoda - Anomura, Brachyura. *In*: Wells A, Houston WWK (eds) Zoological Catalogue of Australia. CSIRO Publishing, Melbourne, Australia 19.3B, 641 pp.

Davie PJF. 2005. A survey of decapod and stomatopod Crustacea of Sweers Island, southern Gulf of Carpentaria. Gulf of Carpentaria Scientific Study Report, Geography Monograph Series 10. Royal Geographical Society of Queensland, Brisbane, Australia, pp. 143–167.

Dayrat B. 2005. Towards integrative taxonomy. Biol J Linn Soc **85:**407–415. doi:10.1111/j.1095-8312.2005.00503.x.

De Grave S. 2001. Biogeography of Indo-Pacific Pontoniinae (Crustacea, Decapoda): a PAE analysis. J Biogeogr **28:**1239–1253. doi:10.1046/j.1365-2699.2001.00633.x.

Doi W, Mizutani A, Kohno H. 2018. Larval release rhythm of the land hermit crab *Coenobita cavipes* Stimpson, 1858 (Anomura, Coenobitidae) on Iriomote Island, Japan. Crustaceana **91:**199–211. doi:10.1163/15685403-00003758.

Fize A, Serène R. 1955. Les Pagures du Vietnam. Institut Océanographique, Nhatrang, Note 45, 228 pp.

Folmer O, Black M, Hoeh W, Lutz R, Vrijenhoek R. 1994. DNA primers for amplification of mitochondrial cytochrome *c* oxidase subunit I from diverse metazoan invertebrates. Mol Mar Biol Biotechnol **3:**294–299.

Goldstein PZ, DeSalle R. 2011. Integrating DNA barcode data and taxonomic practice: Determination, discovery, and description. Bioessays **33:**135–147. doi:10.1002/bies.201000036.

Gong L, Lu XT, Wang ZF, Zhu KH, Liu LQ et al. 2020. Novel gene rearrangement in the mitochondrial genome of *Coenobita brevimanus* (Anomura: Coenobitidae) and phylogenetic implications for Anomura. Genomics **112:**1804–1812. doi:10.1016/j.ygeno.2019.10.012.

Hamasaki K, Fujikawa S, Iizuka C, Sanda T, Tsuru T et al. 2018. Recruitment to adult habitats in terrestrial hermit crabs on the coast of Ishigakijima Island, Ryukyu Archipelago, Japan. Invertebr Biol **137:**3–16. doi:10.1111/ivb.12198.

Hamasaki K, Kato S, Murakami Y, Dan S, Kitada S. 2015. Larval growth, development and duration in terrestrial hermit crabs. Sex Early Develop Aquat Org **1:**93–107. doi:10.3354/sedao00010.

Hamasaki K, Iizuka C, Sanda T, Imai H, Kitada S. 2017. Phylogeny and phylogeography of the land hermit crab *Coenobita purpureus* (Decapoda: Anomura: Coenobitidae) in the northwestern Pacific region. Mar Ecol **38:**e12369. doi:10.1111/maec.12369.

Haswell WA. 1882. Catalogue of the Australian Stalk- and Sessile-eyed Crustacea. Sydney, 324 pp., 4 pls.

Hartnoll RG. 1988. Evolution, systematics, and geographical distribution. *In*: Burggren WW, McMahon BR (eds) Biology of the Land Crabs. Cambridge University Press, Cambridge, pp. 6–54.

Harvey AW. 1992. Abbreviated larval development in the Australian terrestrial hermit crab *Coenobita variabilis* McCulloch (Anomura: Coenobitidae). J Crustacean Biol **12:**196–209. doi:10.2307/1549075.

Heller C. 1865. Crustaceen. Kaiserlich-koniglichen Hof- und Staatsdruckerei, Wien, Austria, 280 pp., 25 pls.

Hoang DT, Chernomor O, von Haeseler A, Minh BQ, Vinh LS. 2017. UFBoot2: Improving the ultrafast bootstrap approximation. Mol Biol Evol **35:**518–522. doi:10.1093/molbev/msx281.

Hoeksema BW. 2007. Delineation of the Indo-Malayan centre of maximum marine biodiversity: the Coral Triangle. *In*: Renema W (ed) Biogeography, Time, and Place: Distributions, Barriers, and Islands. Springer, Dordrecht, The Netherlands, pp. 117–178.

Jones DS, Morgan GJ. 1994. A Field Guide to Crustaceans of Australian Waters. Reed, NSW, Australia, 216 pp.

Kimura M. 1980. A simple method for estimating evolutionary rates of base substitutions through comparative studies of nucleotide sequences. J Mol Evol **16:**111–120. doi:10.1007/BF01731581.

Lanfear R, Frandsen PB, Wright AM, Senfeld T, Calcott B. 2017. PartitionFinder 2: new methods for selecting partitioned models of evolution for molecular and morphological phylogenetic analyses. Mol Biol Evol **34:**772–773. doi:10.1093/molbev/msw260.

Leigh JW, Bryant D. 2015. POPART: Full-feature software for haplotype network construction. Meth Ecol Evol **6:**1110–1116. doi:10.1111/2041-210X.12410.

Lohman DJ, de Bruyn M, Page T, von Rintelen K, Hall R et al. 2011. Biogeography of the Indo-Australian Archipelago. Ann Rev Ecol Evol Syst **42:**205–226. doi:10.1146/annurev-ecolsys-102710-145001.

Malay MCMD, Paulay G. 2010. Peripatric speciation drives diversification and distributional pattern of reef hermit crabs (Decapoda: Diogenidae: *Calcinus*). Evolution **64:**634–662. doi:10.1111/j.1558-5646.2009.00848.x.

McCulloch AR. 1909. Studies in Australian Crustacea. No. 2. Rec Aust Mus **7:**305–314, pls. 88–89.

McLaughlin PA, Komai T, Lemaitre R, Rahayu DL. 2010. Annotated checklist of anomuran decapod crustaceans of the world (exclusive of the Kiwaoidea and families Chirostylidae and Galatheidae of the Galatheoidea) Part I – Lithodoidea, Lomisoidea and Paguroidea. Raffles Bull Zool Suppl **23:**5–107.

McLaughlin PA, Rahayu DL, Komai T, Chan TY. 2007. A Catalog of the Hermit Crabs (Paguroidea) of Taiwan. National Taiwan Ocean University, Keelung, viii+365 pp.

Minh BQ, Schmidt HA, Chernomor O, Schrempf D, Woodhams MD et al. 2020. IQ-TREE 2: new models and efficient methods for phylogenetic inference in the genomic era. Mol Biol Evol **37:**1530–1534. doi:10.1093/molbev/msaa015.

Morgan GJ. 1987. Hermit crabs (Decapoda, Anomura: Coenobitidae, Diogenidae, Paguridae) of Darwin and Port Essington, northern Australia. Beagle Rec Northern Terr Mus Arts Sci **4:**165–186.

Morgan GJ. 1990. A collection of Thalassinidea, Anomura and Brachyura (Crustacea: Decapoda) from the Kimberley Region of northwestern Australia. Zool Verhand Leiden **265:**1–90.

Nakasone Y. 1988 Land hermit crabs from the Ryukyus, Japan, with a description of a new species from the Philippines (Crustacea, Decapoda, Coenobitidae). Zoological Science, Tokyo **5:**165–178.

Ng PKL, Shih HT. 2023. *Tuerkayana latens*, a new species of land crab from French Polynesia, with a discussion on the phylogeny of the genus (Crustacea: Decapoda: Brachyura: Gecarcinidae). Zool Stud **62:**10. doi:10.6620/ZS.2023.62-10.

Padial JM, Miralles A, De la Riva I, Vences M. 2010. The integrative future of taxonomy. Front Zool **7:**16. doi:10.1186/1742-9994-7-16.

Pante E, Schoelinck C, Puillandre N. 2015. From integrative taxonomy to species description: one step beyond. Syst Biol **64:**152–160. doi:10.1093/sysbio/syu083.

Rahayu DL, Shih HT, Ng PKL. 2016. A new species of land hermit crab in the genus *Coenobita* Latreille, 1829 from Singapore, Malaysia and Indonesia, previously confused with *C. cavipes* Stimpson, 1858 (Crustacea: Decapoda: Anomura: Coenobitidae). Raffles Bull Zool Suppl **34:**470–488.

Ronquist F, Huelsenbeck JP, Teslenko M, Nylander JAA. 2020. MrBayes 3.2 manual. Available at: https://nbisweden.github.io/MrBayes/manual.html. Accessed 20 Jul. 2024.

Ronquist F, Teslenko M, van der Mark P, Ayres DL, Darling A et al. 2012. MRBAYES 3.2: Efficient Bayesian phylogenetic inference and model choice across a large model space. Syst Biol **61:**539–542. doi:10.1093/sysbio/sys029.

Sasaki J. 2023. The Species List of Decapoda, Euphausiacea, and Stomatopoda, all of the World, version 07-8.12. Local Independent Administrative Agency Hokkaido Research Organization, Resources Management and Enhancement Division, Abashiri Fisheries Research Institute, Fisheries Research Department, Hokkaido, Japan, 17923 pp. doi:10.13140/RG.2.2.34899.96800.

Schäfer F. 2020. AQUALOG: Land Hermit Crabs - Distribution, Setting up, Maintenance, Breeding. 2nd edition. Aqualog Verlag, Rodgau, Germany, 160 pp.

Schubart CD. 2009. Mitochondrial DNA and decapod phylogenies: the importance of pseudogenes and primer optimization. Crustacean Issues **18:**47–65.

Siallagan ZL, Sidabalok CM, Islami MM, Mujiono NW, Simon P et al. 2023. Why many Indonesian marine species remain undescribed: a case study using polychaete species discovery. Raffles Bull Zool **71:**337–365. doi:10.26107/RBZ-2023-0026.

Shih HT. 2012. Warrior – The Seashore Crabs of Dongsha Island. Marine National Park Headquarters, Kaohsiung, Taiwan, 159 pp. (in Chinese)

Shih HT. 2020. Crescent Swordsmen – The Seashore Crabs of Dongsha Island. Marine National Park Headquarters, Kaohsiung, Taiwan, 207 pp. (in Chinese)

Shih HT, Cai Y, Niwa N, Yoshigou H, Nakahara Y. 2024. Integrative

taxonomy reveals freshwater shrimp diversity (Decapoda: Atyidae: Neocaridina) from Kyushu and southern Honshu of Japan, with a discussion on introduced species. Zool Stud **63:**18. doi:10.6620/ZS.2024.63-18.

Shih HT, Chang K, Pramono FA, Malay MCMD. 2023a. Morphological and molecular evidence for the identity of two land hermit crabs *Coenobita longitarsis* De Man, 1902 and *C. pseudorugosus* Nakasone, 1988 (Crustacea: Decapoda: Anomura: Coenobitidae). Zool Stud **62:**52. doi:10.6620/ZS.2023.62-52.

Shih HT, Hsu JW, Chang K, Chen MW. 2023b. Taxonomy and phylogeography of the freshwater crab *Geothelphusa tawu* species complex (Crustacea: Decapoda: Potamidae) from southern Taiwan and offshore islets. Zool Stud **62:**37. doi:10.6620/ZS.2023.62-37.

Shih HT, Hsu JW, Li JJ. 2023c. Multigene phylogenies of the estuarine sesarmid *Parasesarma bidens* species complex (Decapoda: Brachyura: Sesarmidae), with description of three new species. Zool Stud **62:**34. doi:10.6620/ZS.2023.62-34.

Shih HT, Naruse T, Schubart CD. 2023d. Molecular evidence and differences in gonopod morphology lead to description of a new species of the freshwater crab genus *Candidiopotamon* Bott, 1967 (Crustacea, Brachyura, Potamidae) from eastern Taiwan. Zookeys **1179:**169–196. doi:10.3897/zookeys.1179.106718.

Shih HT, Ng PKL, Davie PJF, Schubart CD, Türkay M et al. 2016. Systematics of the family Ocypodidae Rafinesque, 1815 (Crustacea: Brachyura), based on phylogenetic relationships, with a reorganization of subfamily rankings and a review of the taxonomic status of *Uca* Leach, 1814, *sensu lato* and its subgenera. Raffles Bull Zool **64:**139–175.

Shih HT, Prema M, Kumar AAJ, Saher NU, Ravichandran S et al. 2022. Diversity and distribution of fiddler crabs (Crustacea: Brachyura: Ocypodidae) around the Arabian Sea. Zool Stud **61:**65. doi:10.6620/ZS.2022.61-65.

Siallagan ZL, Sidabalok CM, Islami MM, Mujiono NW et al. 2023. Why many Indonesian marine species remain undescribed: a case study using polychaete species discovery. Raffles Bull Zool **71:**337–365. doi:10.26107/RBZ-2023-0026.

Springthorpe RT, Lowry JK. 1994. Catalogue of crustacean type specimens in the Australian Museum: Malacostraca. Tech Rep Aust Mus **11:**1–134.

Tamura K, Stecher G, Kumar S. 2021. MEGA11: Molecular Evolutionary Genetics Analysis version 11. Mol Biol Evol **38:**3022–3027. doi:10.1093/molbev/msab120.

Tan MH, Gan HM, Lee YP, Linton S, Grandjean F et al. 2018. ORDER within the chaos: Insights into phylogenetic relationships within the Anomura (Crustacea: Decapoda) from mitochondrial sequences and gene order rearrangements. Mol Phylogenet Evol **127:**320–331. doi:10.1016/j.ympev.2018.05.015.

Thurman CL, Shih HT, McNamara JC. 2023. *Minuca panema* (Coelho, 1972): Resurrection of a fiddler crab species from Brazil closely related to *Minuca burgersi* (Holthuis, 1967) (Crustacea, Decapoda, Brachyura, Ocypodidae). Zool Stud **62:**45. doi:10.6620/ZS.2023.62-45.

Veron JEN, Devantier LM, Turak E, Green AL, Kininmonth S et al. 2009. Delineating the Coral Triangle. Galaxea JCRS **11:**91–100. doi:10.3755/galaxea.11.91.

Wáng FJ. 2006. Kelomang Darat (Land Hermit Crab). Happy Crabbie, Jakarta, 68 pp. (in Indonesian)

Wang Q, Lia YJ, Tang D, Wang J, Xua JY, Xua XY, Wang ZF. 2019. Sequencing and analysis of the complete mitochondrial genome of *Coenobita brevimanus*. Mitochondrial DNA B **4:**2645–2646. doi:10.1080/23802359.2019.1643801.

Will KW, Mishler BD, Wheeler QD. 2005. The perils of DNA barcoding and the need for integrative taxonomy. Syst Biol **54:**844–851. doi:10.1080/10635150500354878.

Yuan ZM, Jiang W, Sha ZL. 2022. A review of the common crab genus *Macromedaeus* Ward, 1942 (Brachyura, Xanthidae) from China Seas with description of a new species using integrative taxonomy methods. PeerJ **10:**12735. doi:10.7717/peerj.12735.